Research and Development Progress Report No. 290 • January 1968

The Piston Bed and its Design

By H. F. Wiegandt, R. L. Von Berg and J. P. Leinroth, Cornell University, for Office of Saline Water, J. A. Hunter, Director; W. Sherman Gillam, Assistant Director, Research; Sidney Johnson, Chief, Applied Science Division

UNITED STATES DEPARTMENT OF THE INTERIOR • Stewart L. Udall, Secretary
Frank C. Di Luzio, Assistant Secretary for Water Pollution Control

For sale by the Superintendent of Documents, U.S. Government Printing Office, Washington, D. C. 20402 — Price 40 cents

Created in 1849, the Department of the Interior—America's Department of Natural Resources—is concerned with the management, conservation, and development of the Nation's water, wildlife, mineral, forest, and park recreational resources. It also has major responsibilities for Indian and Territorial affairs.

As the Nation's principal conservation agency, the Department of the Interior works to assure that nonrenewable resources are developed and used wisely, that park and recreational resources are conserved for the future, and that renewable resources make their full contribution to the progress, prosperity, and security of the United States—now and in the future.

FOREWORD

This is one of a continuing series of reports designed to present accounts of progress in saline water conversion and the economics of its application. Such data are expected to contribute to the long-range development of economical processes applicable to low-cost demineralization of sea and other saline water.

Except for minor editing, the data herein are as contained in a report submitted by the contractor. The data and conclusions given in the report are essentially those of the contractor and are not necessarily endorsed by the Department of the Interior.

TABLE OF CONTENTS

	Page
ABSTRACT	
INTRODUCTION	1
DEVELOPMENT OF ANALOGY	5
INTERPRETATION OF V_g	10
THE ELECTRICAL ANALOG	15
ESTABLISHING THE BRINE CROWN	27
DESIGN EXAMPLES	32
ACKNOWLEDGEMENT	51
LITERATURE CITED	56

LIST OF FIGURES

Figure		Page
1.	Hydraulic Force Representation of Piston Bed. Vertical Flooded Bed.	6
2.	Hydraulic Force Representation of Piston Bed. Horizonatl Bed; Flooded Bed.	6
3.	Hydraulic Force Representation of Piston Bed. Horizontal Bed; Flooded Bed; Wall Friction	8
4.	Circuit Diagram for Column Evaluation	17
5.	Analysis of Analog	19
6.	Analysis of Analog	24
7.	Analysis of Analog	25
8.	Designs I, I-A, II, III	35
9.	Designs IV, V, VI	37
10.	Designs VII, VIII, IX	41
11.	Designs X, XI	43
12.	Designs XII, XIII	47

LIST OF FIGURES

(Continued)

Figure		Page
13.	Designs XIV, XV	49
14.	Designs XVI, XVI-A	53
15.	Designs XVII, XVIII	55

TABLE

Table 1	Estimated Values of $-v_g$	13

ABSTRACT

The piston-bed column has been used extensively for countercurrent washing of solids. An electrical analog technique is developed and then applied to eighteen variations of rectangular piston-bed columns to illustrate this method of analysis.

The piston bed is viewed simply as a moving, porous bed acting as a free piston which is constantly being cut off at one end and replenished at the other. For a vertical column containing an upwardly moving ice bed, a drainage port is provided at an intermediate level. In a properly operating column, brine flows upward and wash water downward, each toward the drainage port; and washed ice is removed. A good design permits recovery of washed ice with little net loss of water for washing.

The analogs permit a rapid and accurate appraisal of a conceptual design. Examples of both pressure and streamline analogs show the broad utility of the method.

A dimensionless ice velocity, V_i, is used to characterize column performance. It is the ratio of the actual ice velocity to whatever lineal, gravity, drainage-rate of water is characteristic for the bed in question. Thus definitive designs are possible without the requirement for empirical knowledge of the crystal system.

Of the designs presented the lowest V_i is 0.56 and the highest is 1.83. Advantages result from the use of contoured top surfaces, wide drainage-ports, unflooded drainage-ports, and hydraulic forces greater than gravitational to achieve ice rates much higher than those possible in early designs.

The relationship between the crystallization step and washing may be significantly influenced by improved piston-bed columns.

INTRODUCTION

All freezing processes or hydrate processes for desalination employ a freezing step which produces a slurry of crystals in a waste brine having a salt concentration greater than that in the crystallizer feed. An essential process requirement is the almost complete separation of these crystals from the brine.

One method to achieve this separation is with a hydraulic-piston bed (12) in which brine flows upward cocurrently with the suspended crystals, the crystals add to the bottom of an upwardly moving crystal bed, a displacement head of fresh water flows from the top with a very small downward component, and both streams exit through a drainage zone flush to the moving ice bed and intermediate to the top and bottom. Schematic representations are presented later in the report. The operation of a hydraulic-piston bed permits substantially increased rates over those dependent on ice buoyancy alone.

Early analyses of bed hydraulics were made by Bosworth, Barduhn, and Sandell (3), and in these laboratories by Wiegandt (12). In the latter study an approximate analysis was made to determine the slip between ice and brine as a function of particle diameter and lineal ice rate. The ice rate was assumed to be equal to the full gravity-drainage rate of water flowing through the bed. This ice rate was considered as the maximum that could be achieved for a deep bed operated with a liquid level below the top of the bed. A recent design of a piston-bed column for a pilot plant is included in a report by Johnson, Moore, Wagaman, and Sandell (6). Their report refers to a design method which W. Hahn presented at a symposium in Los Angeles, November, 1965. The same assumption of full gravity flow in the washing zone was made by Johnson, et. al. (6) as by Wiegandt (12). It will be shown later in this report that this assumption is optimistic.

When using positive washing forces, in flooded-bed operation, to achieve rates greater than those possible from a draining-bed operation, the optimum relationship between crystallizer size and piston-bed design will be affected. It is a purpose of this report to present a number of design alternates and to show the extent to which bed rates can be increased. At Reynolds numbers (based on particle diameter) substantially less than 10, the flow rate through the bed can be assumed proportional to the pressure drop as represented by Darcy's Law, and the pressure drop can be expressed by classical methods of fluid dynamics. Bosworth, Barduhn, and Sandell (3) presented the integrated equation for pressure drop for a washer which used a conical section for upflow followed by a cylindrical

section with a horizontal annular screen at its bottom to carry out the brine and the net downflow of wash water. The behavior of the piston bed has been interpreted according to the concept (2) that the vertical movement of the ice bed results from the frictional forces between the flowing brine and the porous mass of crystals.

The concept adopted in the 1960 publication (12) and applied again in this report is that the piston bed may be visualized as a free piston with a force applied at the top and at the bottom. To move the piston upward and to overcome the wall friction, a small additional force is required at the bottom. The flow of liquid through the piston is dependent on the fact that the piston is porous. It is thus convenient to think of water and brine as leaking through the porous structure from each end toward an intermediate drainage zone.

The two principal features of this analysis of a piston bed can be considered quite independently: (1) the balance and movement of the bed resulting from the opposed forces; and, (2) the hydraulic flow of liquid (relative to the bed) toward the drainage zone as influenced by the magnitude of these forces and by the geometry and permeability of the bed. The summation of the local vertical drag forces within the bed are numerically equal to the total applied forces. A lateral directional component of flow thus is of no significance in the vertical force balance (except as it may influence wall friction). but it will be seen later in this report that the flow pattern affects greatly the leakage rate of the streams into the bed.

It should be recognized that there is a zone of consolidation as the bed forms and the assumption of a compacted piston will be represented in a real operating column by a piston having some additional depth. Other methods of analysis must, of course, also take account of the fact that a changing porosity exists. This consolidation which takes place after the particles are in loose contact would seem (based on visual observation of bed formation in six-inch diameter columns) to contribute to randomness of bed structure. A laboratory column of a small cross section might be different in this respect from a large pilot plant or commercial column.

References to other considerations of the behavior of piston bed columns and ice washing are given by Sherwood, Brian, Sarofim and Smith (11). The very limited amount of intermixing or dispersion between the liquids in the displacement of brine by wash water was determined experimentally by Karnofsky (8) and by Leinroth, White, Sherwood and Brian (9).

Karnofsky reported displacement washing of a flooded fixed bed with operation at the maximum possible rate as allowed by gravity drainage through a bottom screen which supported the bed. The break-through data showed that substantially less than 10 percent of the

final product would be lost in displacement washing. Karnofsky also noted that a small decrease in bed porosity resulted from the additional ice which forms as 32°F wash water contacts colder ice. The ice which originally forms the bed is at the equilibrium freezing temperature of the brine. The extent to which this supplemental freezing (about 2.5% of additional ice at 50% conversion) contributes to the washing effectiveness has not been established. It represents a case of unsteady-state heat transfer for each individual crystal. The resulting washed bed is entirely different in character from the bed as originally formed from the brine slurry and may be described as a strong, monolithic, porous solid.

To obtain meaningful data for large units by measuring pressure profiles both in cross-section and longitudinally in a small experimental moving bed is very difficult because of the short horizontal distances, because of problems created when the bed becomes hard and rigid in the wash zone, because of the relative magnitude of the upward force required to overcome wall friction, and because of the difficulty of reproducing the same crystal size distribution for the various different operating tests. In one process study (12), the wall friction was minimized by using a conical column having a taper of about 4°. Tapered columns are not sufficiently representative of vertical columns actually used to permit reliable scale-up, although these tests did establish the feasibility of the piston-bed concept. In a cylindrical column six inches in diameter, a significant portion of the driving force applied at the bottom was dissipated in overcoming wall friction. With larger columns in pilot plant operation the wall friction is of minor significance.

A similar experience was encountered in a pilot plant development for producing paraxylene (13). The scale of operations was such that the piston-bed purification of paraxylene crystals was conducted in a conical column for easy movement of the bed through the column.

Brandt and Johnson (4) made a study of the extent to which resistance to bed movement develops with ion-exchange particles, also in comparatively small columns. The coefficient of friction was not the same for the regenerated and loaded resin. Similarly one can expect the wall friction for ice beds to vary depending on the wall material. Finally, a special experimental complication exists for ice beds in small insulated columns whereby local pressures may constantly be relieved by a small amount of melting.

A computer solution was worked out by Mixon (10) for a specific example of a piston-bed column. Some of the input information required for the programming, such as ice velocity and brine velocity cannot be provided for exploratory designs. His work is intended primarily to analyze the performance of existing columns from which operating data are available.

The present report develops the use of an electrical analog in which the conceptual column geometry of rectangular columns is represented on resistance paper. The original plan for making a simulation hydraulically in a fixed bed was dropped when it became evident that an electrical analog is more accurate, more flexible, and provides more information. The objective is to have a design method which is simple, rapid, correct, and which allows a clear visualization of the actual process equipment that can be utilized. The contributions to creative improvements from such an approach are self-evident, and it is hoped that the designs developed in the report will serve as a basis for additional future design improvements.

DEVELOPMENT OF ANALOGY

The limitations in the use of operating data from small experimental units as a basis for scale-up of piston beds has been described. The difficulties of interpreting operating data from a pilot-plant in order to design greatly modified units may make some pilot-plant studies restrictive to innovative flexibility.

Fortunately the predictable characteristics of fluids flowing at low Reynolds numbers through porous beds permits the use of an electrical analog which gives clear, quantitative representations of new designs. When a particularly advantageous analog has evolved, the proof of its qualities must, of course, be established in a real pilot test. However, the economies of achieving such a design by an easy method will hopefully contribute to the realization of the potential advantages of the freezing process.

In Figure 1 is shown a buoyancy bed. It illustrates the hydraulic balance in manometer representation between the slurry feed and the ice column. The buoyancy of the ice will cause the ice to rise very slowly; so slowly, in fact, that its contribution is considered zero for practical columns. If a drainage zone is provided in the wall of this column, liquid will proceed to flow through it. However, in the absence of wall friction, the manometer on the slurry line remains unchanged if the wash liquid is maintained exactly at the top of the column. Now, if ice is provided by the slurry such that the upward movement of ice equals the lineal flow rate of wash water down through the ice, the wash water is stationary to the observer and the operation of a piston bed, as represented in Figure 1, has been achieved.

The hydraulics of a piston bed may also be visualized for a horizontal bed with the advantage for discussion purposes that in the horizontal zone gravity forces need not be considered. If the piston bed in Figure 1 is laid on its side it can be represented as in Figure 2.

The following conditions are specified:

FIGURE 1

HYDRAULIC FORCE REPRESENTATION FOR PISTON BED
Vertical Flooded Bed

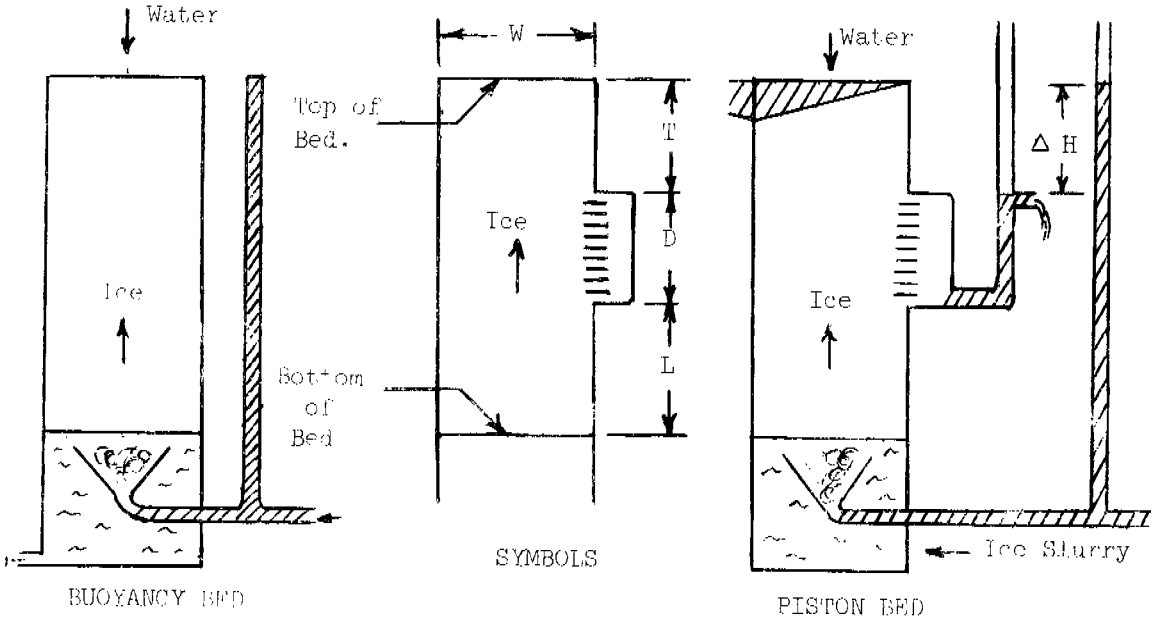

FIGURE 2

HYDRAULIC FORCE REPRESENTATION FOR PISTON BED
Horizontal Bed; Flooded Bed Operation.

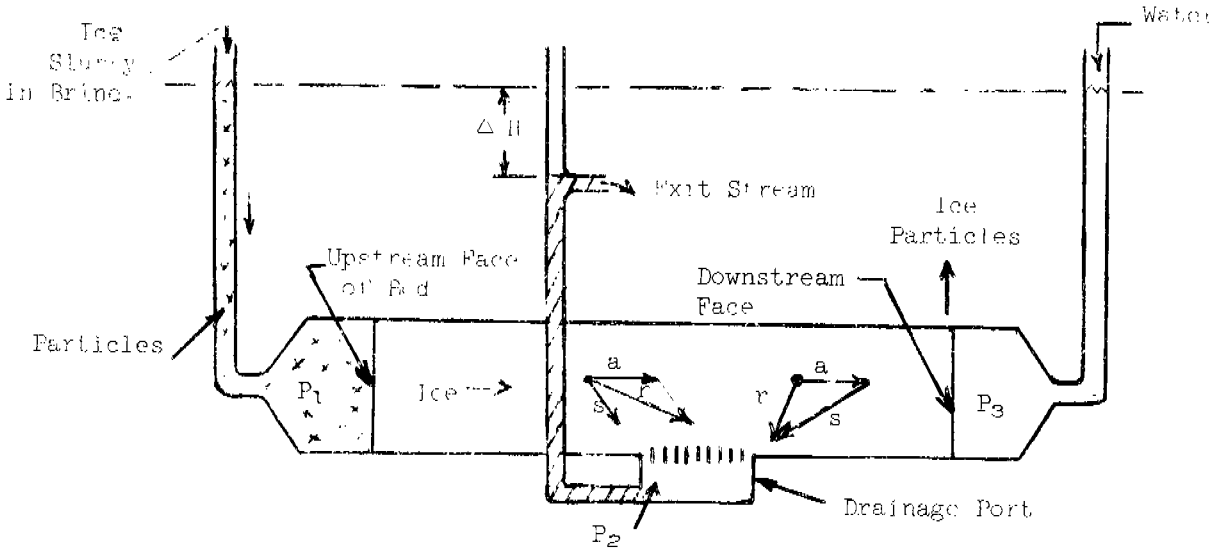

1. The brine with suspended ice particles enters the bed at pressure P_1.

2. The ice particles add to the upstream face of the moving bed. The face position remains stationary to the observer.

3. Ice particles free of liquid are eliminated from the downstream face by some fictitious means. The face position remains stationary to the observer.

4. Water is available at the upstream end at pressure P_3.

5. An exit stream which represents the total brine plus water input leaves the drainage port at pressure P_2. Pressure P_2 is less than either P_1 or P_3.

6. The bed is uniformly structured, and there is no wall friction.

The following observations may be made:

1. Flow rates relative to the bed are established by P_1, P_2, and P_3.

2. In the absence of wall friction, P_1 must always be exactly equal to P_3 or the entire bed position will move in the direction of lower pressure.

3. The pressure at any specified point in the bed is the same for any uniformly structured bed.

4. Pressures at all points in the bed (i.e. fixed points to the observer) remain constant whether the bed is moving or not.

5. It follows from 4 that all flows relative to the bed remain the same whether the bed is moving of not.

6. Actual velocity flow vectors (to the observer) are thus the vector sum of the flow-rate vectors (shown as s) for the stationary bed and the axial rate contribution (shown as a) to give the actual, resultant flow vector (shown as r). The axial rate is the lineal rate of the bed.

If there is a significant resistance to bed movement, perhaps because of wall friction, Figure 2 is in error. However, rather than to introduce such effects as wall friction, bed consolidation, buoyancy, etc. into the basic analysis, and thereby complicate it, the bed length at the feed end can be adjusted to compensate. It will be observed later that the constant pressure lines for a large initial portion of the upstream ice bed are essentially perpendicular to the axial-flow direction of the bed. Thus, in a real bed the constant pressure line, P_1, will be as shown by Figure 3.

FIGURE 5

HYDRAULIC FORCE REPRESENTATION OF PISTON BED

HORIZONTAL BED; FLOODED BED; WALL FRICTION

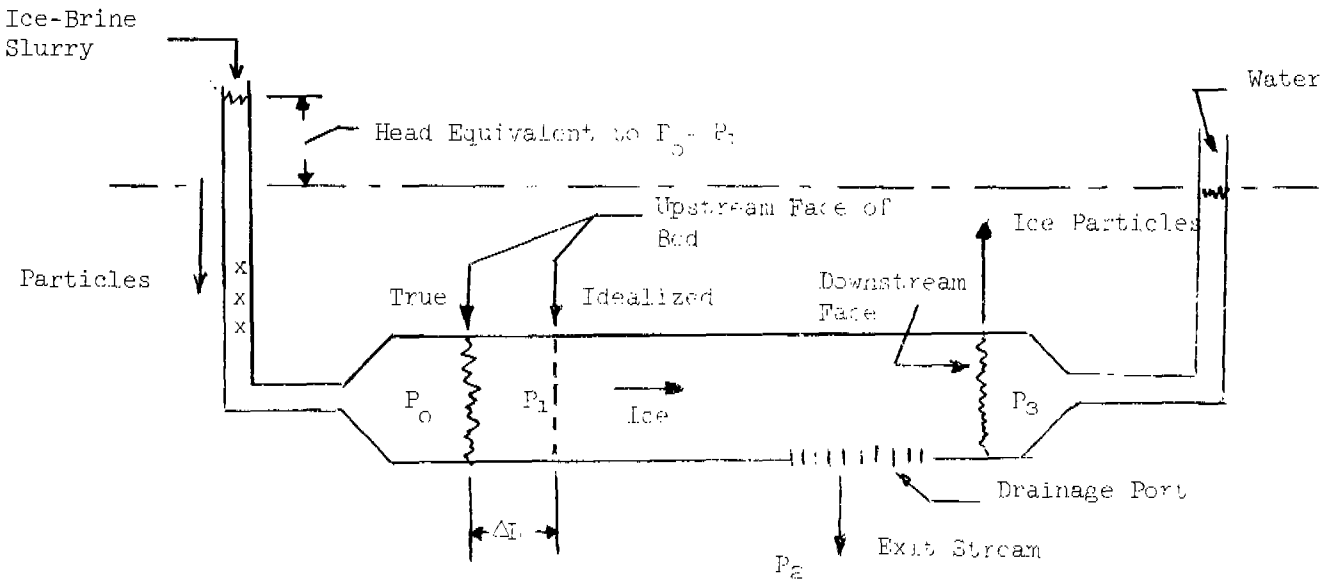

With this major simplification it becomes possible to think of flooded horizontal ice beds in which there always exists a P_1 which is equal to P_3, and this (in terms of hydraulic potentials for beds which are vertical) is done in the design considerations which follow in this report. A distance, ΔL, will be provided for an engineered design, and it merely represents the additional bed depth which allows for all the non-idealities. In the remainder of this report ice columns are considered as extending from the idealized upstream face to the downstream face and the force balance of a horizontal column is with P_1 equal to P_3.

It now becomes obvious that once a column geometry has been fixed the lineal ice rate must fall between zero and some maximum which will still permit a brine-water "interface" to exist. Within allowable ice rates, this interface for a properly proportioned column must exist when there is a small, positive flow of water through some cross-section of the column, not necessarily planar, between the downstream face and the drainage port. With P_3 fixed, the flow of wash water can be regulated by adjusting P_2.

Another major simplification to the designer is to avoid the empirical properties of a specific ice bed as an input requirement to the design method. Karnofsky (7) suggested (and this is for vertical beds) the use of a dimensionless ice velocity, V_i, which is the ratio of the lineal rate, v_i, of a specific ice bed to the full lineal gravity-drainage rate, v_g, of water in axial flow through the identical bed, or

$$V_i = \frac{v_i}{-v_g}$$

where

V_i = dimensionless velocity

v_i = upward ice velocity, ft/min

v_g = lineal gravity-drainage rate, ft/min

INTERPRETATION OF v_g

The full lineal gravity drainage rate, v_g, can also be referred to as the slip rate of water in ft./min. under the conditions of gravity drainage down through a stationary bed and with no exit restrictions. There are numerous representations of flow through porous media which refer to permeabilities, equivalent diameters, superficial velocities, porosities, etc., in both metric and English units. In most hydraulic representations the velocity is a superficial velocity because the interest is in the quantity of liquid which will flow through a bed. In a washing bed it is the slip rate which is desired because the concern is with how fast the bed itself may be moved.

The slip rate in viscous flow is proportional to the applied force and is expressed

$$v = K_B \frac{\Delta P}{Z}$$

where

v = slip rate, ft/min
K_B = proportionality constant, $\frac{ft^4}{lb_f\ min}$
ΔP = pressure differential, lb_f/ft^2
Z = length of porous bed, ft

and for full gravity flow

$$v_g = -K_B \rho \frac{g}{g_c}$$

where

v_g = lineal gravity-drainage rate or slip rate with gravity flow, ft/min
ρ = density, lb_m/ft^3
g = acceleration of gravity, 32.2 ft/sec^2
g_c = dimensional constant, 32.2 $\frac{lb_m\ ft}{lb_f\ sec^2}$

To relate to the superficial velocity, based on the total cross section of the bed as is used in many equations, a conversion involving the porosity (e) is required.

Hence

$$v_{superficial} = K_B \frac{\Delta P}{Z} e$$

and

$$v_{g\ superficial} = -K_B \rho \frac{g}{g_c} e$$

where

$v_{superficial}$ = velocity of liquid based on cross section of bed,

e = porosity or void fraction, ft^3/ft^3

As used by Hahn, et al, (5) in terms of permeability, B_o, in the metric system

$$\frac{Q}{A} = v_{superficial} = \frac{B_o g h}{\mu L}$$

and

$$v_{g\ superficial} = \frac{B_o \rho g}{\mu}$$

and in terms of slip rate as used in the present report

$$-v_g = \frac{B_o \rho g}{e \mu}$$

where

Q = flow rate, cm^3/sec
A = bed cross section, cm^2
$-v_g$ = slip rate, full gravity flow, cm/sec
B_o = permeability constant, cm^2
ρ = fluid density, gm/cm^3
g = acceleration of gravity, cm/sec^2
h = head loss, cm
L = bed length, cm
μ = viscosity gm/cm sec
e = porosity, cm^3/cm^3

With v_g as defined in the present report it is equally correct to consider the slip rate of water at full gravity flow down through the bed or to think of v_g as the lineal upward rate of ice when the water by gravity forces remains stationary to the observer. For this comparison, when v_i, the lineal ice rate, is numerically equal to v_g, then V_i, the dimensionless ice velocity, is equal to one. In referring to this corresponding lineal ice movement when using the permeability formula, the porosity must be included such that for true volumetric rate

$$\text{Ice production, } \frac{Ft^3}{Ft^2 min} \text{ of 100\% ice} = \frac{B_o \rho g}{\mu} \cdot \frac{(1-e)}{e} \cdot \frac{1.97\ ft/min}{1 cm/sec} \cdot V_i$$

In the present report the emphasis is on geometries which influence V_i. It should be noted, however, that the ultimate objective is to have a maximum production rate of ice. Since

$$V_i = \frac{v_i}{-v_g}$$

or

$$v_i = V_i\ (-v_g)$$

then (using actual and not superficial velocities)

Production, $lbs/ft^2 min = v_i\ (1-e)\ \rho = V_i\ (-v_g)(1-e)\rho$

where

V_i =dimensionless velocity

v_i =ice velocity, ft/min

$-v_g$ =slip rate, gravity flow, ft/min

ρ =absolute density of ice, lbs_m/ft^3

e =porosity or void fraction, ft^3/ft^3

From the Carmen-Kozeny relationship: for constant porosity v_g is proportional to d_p^2 and for constant particle size v_g is proportional to $(\frac{e}{1-e})^2$. It is thus evident that for 10% increase in the equivalent particle diameter, for example, all other things remaining constant, the relative maximum ice production will be $(\frac{1.10}{1})^2$ or increased by 21%. On the other hand, by increasing the bed porosity from 0.50 to 0.55 all other things remaining constant, the relative maximum ice production will be $(\frac{0.55}{1-0.55})^2\ (1-0.55)/(\frac{0.5}{1-0.5})^2(1-0.5)$ or increased by 34%. Obviously the equivalent particle diameter and the bed porosity, are both important to the overall freezing process. The crystallization step has an important causal relationship to the magnitude of v_g. Crystallizer design is not considered in this report. Substantial improvements have already been achieved in pilot-plant crystallizers, and crystallization is being further studied in these and other laboratories.

There are few published data which permit the prediction of v_g. Barduhn (2) gave some production figures. Using as examples these numbers and also the design value of permeability, B_o, of $1 \times 10^{-6}\ cm^2$ as proposed by Johnson, et al. (6), the v_g values are estimated for an assumed porosity of 0.5 as indicated in Table 1.

TABLE 1.

Estimated Values of $-v_g$

Column	Ice Production Lbs/hr ft^2 (2)	v_i (e=0.5, assumed) Ft/min	V_i (assumed)	$-v_g$ Ft/min
Cornell - Blaw Knox	700	0.38	0.7	0.55
Colt	300	0.16	0.7	0.23
Carrier	165	0.090	0.7	0.13
OSW Column	1000	0.55	0.7	0.79
Carrier (Proposed)	$B_o = 1 \times 10^{-6}$ cm^2 (6)			0.183

The assumption of a bed porosity of 0.5 may, of course, be far from valid, and more will be said about v_i. The relationship of column design to bed porosity is a topic that requires more attention. A few comments can be made at this time, but the exact answers must await the results of future experiment. Hahn, et al, (5) have already suggested that drain-plate design, brine flow rate, and particularly the load of the column affect the porosity. They and Johnson, et al, (6), refer to a standardized permeability test for characterizing crystallizer products. While extremely useful for this purpose, the permeability test, however, might not predict the behavior of ice in a specific piston-bed column. One variable, possibly very important, is the bed depth below the drainage port. A deep forming-bed will have a low brine slip-rate; it will also structure gradually with a slow progressive compaction. No information exists on bed porosities for different total loads as influenced by the dynamics of ice-bed formation, especially for columns large enough to minimize wall effects.

The comparison in Table 1 is not only an estimate, but it makes no distinction regarding whether the piston bed is being operated as a flooded bed (i.e. the liquid level extends to the top of the column) or as a partially drained bed (i.e. the liquid level is below the top of the ice and the contour of the upper surface of the wash-water phase adjusts itself according to the geometry of the column, the characteristics of the bed, and the operating conditions). The complex hydraulics of a partially drained bed is beyond the scope of this report. However, a draining bed can never transmit as much water as can a flooded bed. Thus, the values for v_g probably should be numerically greater than indicated in Table 1, and for the same V_i of 0.7 the ice production rates (which as listed are for partially-drained beds) could have been greater had the bed been operated flooded. On the other hand, the wide range of values for v_g does not necessarily mean that the information is

inconsistent. Both Colt and Carrier used vacuum freezing for their crystals; the OSW column and the Cornell-Blaw Knox column received crystals produced by vaporizing a hydrocarbon from the slurry; Carrier (proposal) uses a fluorocarbon. A rather wide range of crystal sizes is to be expected, especially as further influenced by the design and operation of specific crystallizers.

The chief concern with flooded bed operation is the wash-water loss. There is no self-developing liquid contour as in draining-bed operation to establish minimum wash-water loss. There is by necessity (for a flooded bed having a flat, horizontal ice-surface) an excess of downward wash-water flow along those vertical surfaces which have drainage ports if at the same time the required washing is achieved in the interior of the bed. Hahn, et. al. (5) reported that flooded-bed operation is technically feasible and that higher ice rates are possible with this mode of operation. The average net wash (per cent of gross product) ranged from 10.6 to 28.5% in their tests.

It will be shown later in this report that with columns of proper design flooded beds may be subject to very small wash-water demands. Insofar as the present objective is to advance the designs of piston-bed columns in the direction of those which promise greater thruput, and this is the case for flooded operation, there is an immediate purpose to develop specifically a design method for the flooded bed.

THE ELECTRICAL ANALOG

The hydraulic force representation of a horizontal bed as in Figure 3 was for discussion purposes. For representation of a vertical bed, potentials are used. This point, although elementary, must be made very clear. All potentials, expressed hydraulically as lb_F/ft^2 (or for convenience the equivalent feet of head) and electrically as voltage, are in reference to a common datum plane. In other words, an open column of liquid has the same potential over its length because manometers inserted at any level would show a liquid level exactly the same as that of the column. If liquid maintained at the same column liquid level were flowing downwardly through this column and through a restrictive orifice plate in the column, a manometer inserted at a level below the orifice plate would register a liquid level lower than in the column. The difference in levels is the loss in potential. Thus, for porous beds when Darcy's law applies

$$v_z = - K_B \left[\frac{\partial}{\partial z} \left(P + \rho \frac{g}{g_c} z \right) \right]$$

$$v_x = - K_B \left[\frac{\partial}{\partial z} \left(P + \rho \frac{g}{g_c} z \right) \right]$$

or

$$v_z = - K_B \frac{\partial}{\partial z} \left[\phi \right]$$

$$v_x = - K_B \frac{\partial}{\partial x} \left[\phi \right]$$

where

v = slip velocity, ft/min

P = static pressure, lb_F/ft^2

ρ = density, lb_M/ft^3

z = vertical coordinate, ft.

x = horizontal coordiante, ft

$\phi = \left(P + \rho \frac{g}{g_c} z \right)$ = potential, lb_F/ft^2

In terms of an electrical analog, ϕ is the voltage and the column is a geometrical representation which is made from resistance paper (Western Union Teledeltos paper).

Additional examples of using an electrical analog technique are discussed by Albright (1) for fluid flow, heat flow, and diffusion. He does not give references to other literature.

At openings in the column, ϕ can be evaluated as a boundary condition and imposed on the proper parts of the resistance paper. All column dimensions are relative and all voltages are determined as percentages of battery voltage. On this basis all flow rates can be determined in dimensionless parameters and can apply to any column of the same geometry and relative imposed hydraulic potentials.

The values of ϕ may be determined for a particular situation and applied to this analog. The result of such an analog will be a series of constant voltage lines equivalent to constant hydraulic potential lines which represent the conditions in a stationary bed for the imposed boundary conditions. It will be shown later how an analog may be constructed directly for a moving bed.

Figure 4 is a diagram of the electrical circuit system and a representative column. Equal voltage is supplied to the ends of the column (representing $P_1 = P_3$ as in Figure 3, or equal hydraulic potential between the top of the bed and the idealized bottom face of the bed) from one terminal of a standard 12 volt storage battery. The ends of the resistance paper are painted with conductive paint. If the piston bed is represented by a flooded drain (as P_2, or constant hydraulic potential, in Figure 3), a conductive line is provided for the drain opening, D, and contact is made directly to the other terminal of the battery. If the representation is for an open drain (and Figure 4 shows this representation) such that the liquid pours directly into a vapor space, the pressure represented in the vapor space would logically be either the same as the pressure of the vapor above the column or preferably a lower pressure such as the operating pressure of the crystallizer. For the open drain a calculated, predetermined, linear voltage-gradient is approximated with an initial terminal contact at the base of the drain plus ten additional contacts at equal-voltage increments connected over the length of the drain. A simple trial and error adjustment of the terminal arrangements along the drain can, because of the interaction with the other electrical flows in the paper, make the gradient almost perfectly linear. A small lip of Teledeltos paper is retained along the length D to facilitate the linearization. The voltage desired for the top of the drain (predetermined as discussed later) is set with a variable resistance. A sensitive, light-beam galvanometer shows zero deflection when the probe contacts a point on the paper which balances the setting on the voltage divider. Not shown in the diagram is the sensitivity circuit to protect the galvanometer during the null-point search.

FIGURE 4

CIRCUIT DIAGRAM FOR COLUMN EVALUATION

CONSTANT PRESSURE LINES

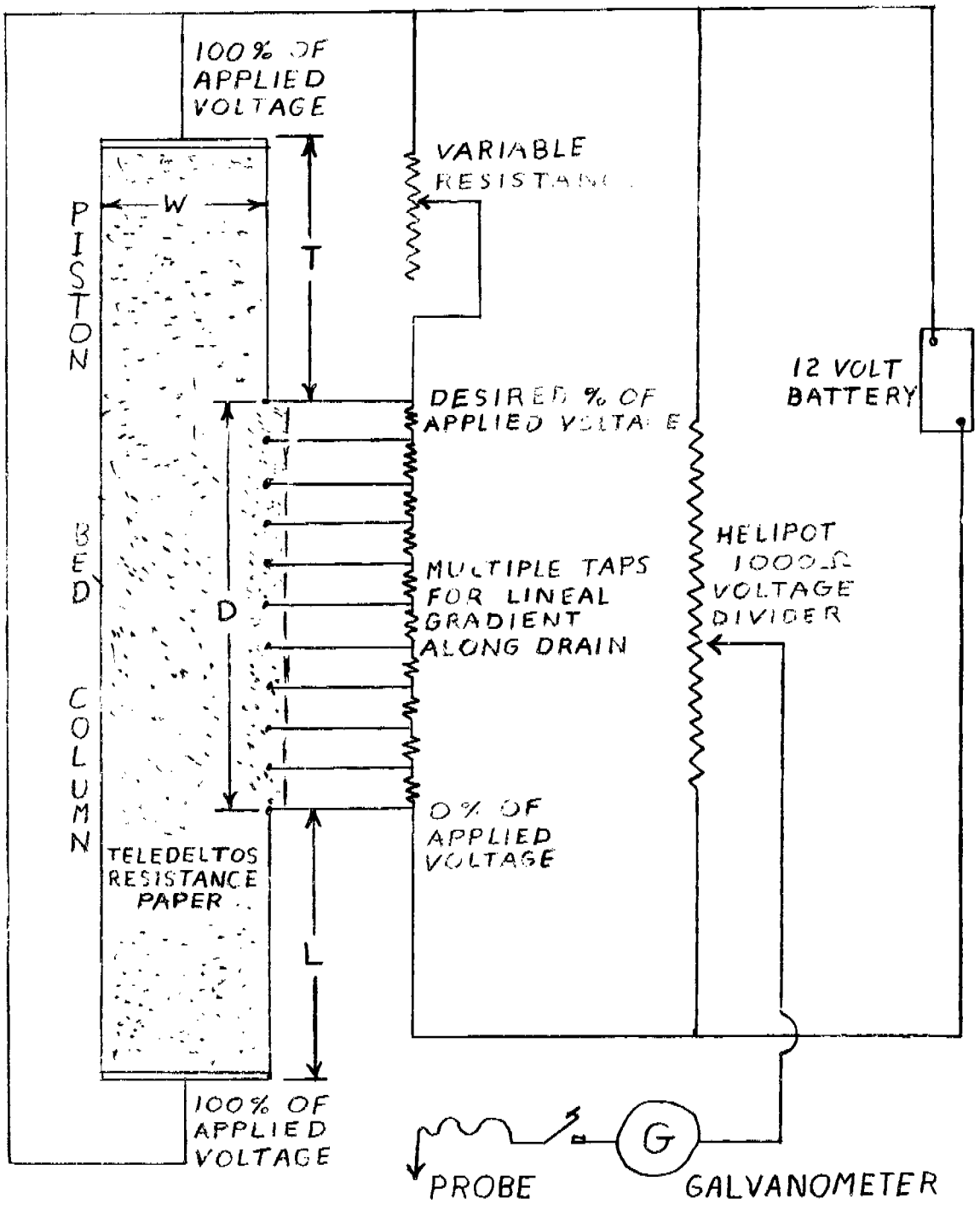

In Figure 5 is shown part of an analog diagram to illustrate the first steps in the analysis. The half-column represents an ice bed with a V-shaped top surface in which the V is filled with wash water. A flooded drain is held with a back pressure (at the top of the drain) which is the same as the pressure above the column.

The top of the bed is at uniform hydraulic potential and, thus, the total applied voltage assigned the value 100%, extends along this surface. The drainage port is at a constant and at the lowest hydraulic potential and, thus, is assigned the value of 0%.

The gravity-drained bed used as a comparison standard for this example is represented as extending from the same elevation for top liquid-level to the level of the outflow. The hydraulic potential loss (in this case equal to the static pressure loss) in such a bed is uniform and the appropriate 10% lines (the increments selected for this illustration) are equi-spaced.

Although actual flow rates cannot be expressed from the diagram, the relative flow rates are inversely proportional to the distance, h, between a selected potential increment, in this case 10% of the total potential. The units for measurement of h are at the convenience of the person making the analysis because they are all relative and cancel out in establishing the V_i. For example in these laboratories the analog paper representing Figure 5 had W = 4 inches, T = 8 inches, etc., and the distances between constant potential lines of 10% increments (5% increments was the basis for many analyses) were measured in hundredths of inches. Thus 1/h for $-v_g$ is 1/0.80 in the original full-scale representation of Figure 5.

For the column in Figure 5 it is immediately evident that the flow pattern relative to the upper part of the bed is complex and sweeps from the slanted top surface in a combination cross and downflow. However, any number of vertical section-lines can be drawn and the vertical component of flow, $-v_z$, relative to the bed can be represented by 1/h for any 10% increment. Where the potential lines are not equidistant the obvious errors of working with delta increments rather than differential quantities exist, but, as will be seen, the controlling measurements concern lines that are essentially equidistant, and this easy method of analyzing the diagram can be justified. It is necessary only to exercise judgment in selecting voltage increments for plotting such that one obtains accuracy for linear measurements consistent with representative distances (delta measurements) for the controlling measurements.

For each of the vertical section-lines drawn, there will be in the washing zone one vertical increment (between constant potential lines)

FIGURE 5

ANALYSIS OF ANALOG

Representation of Voltage Increments to Establish Relative $-v_g$ and $v_{i\ max}$. Pressure at top of Drainage Port = Pressure above column.

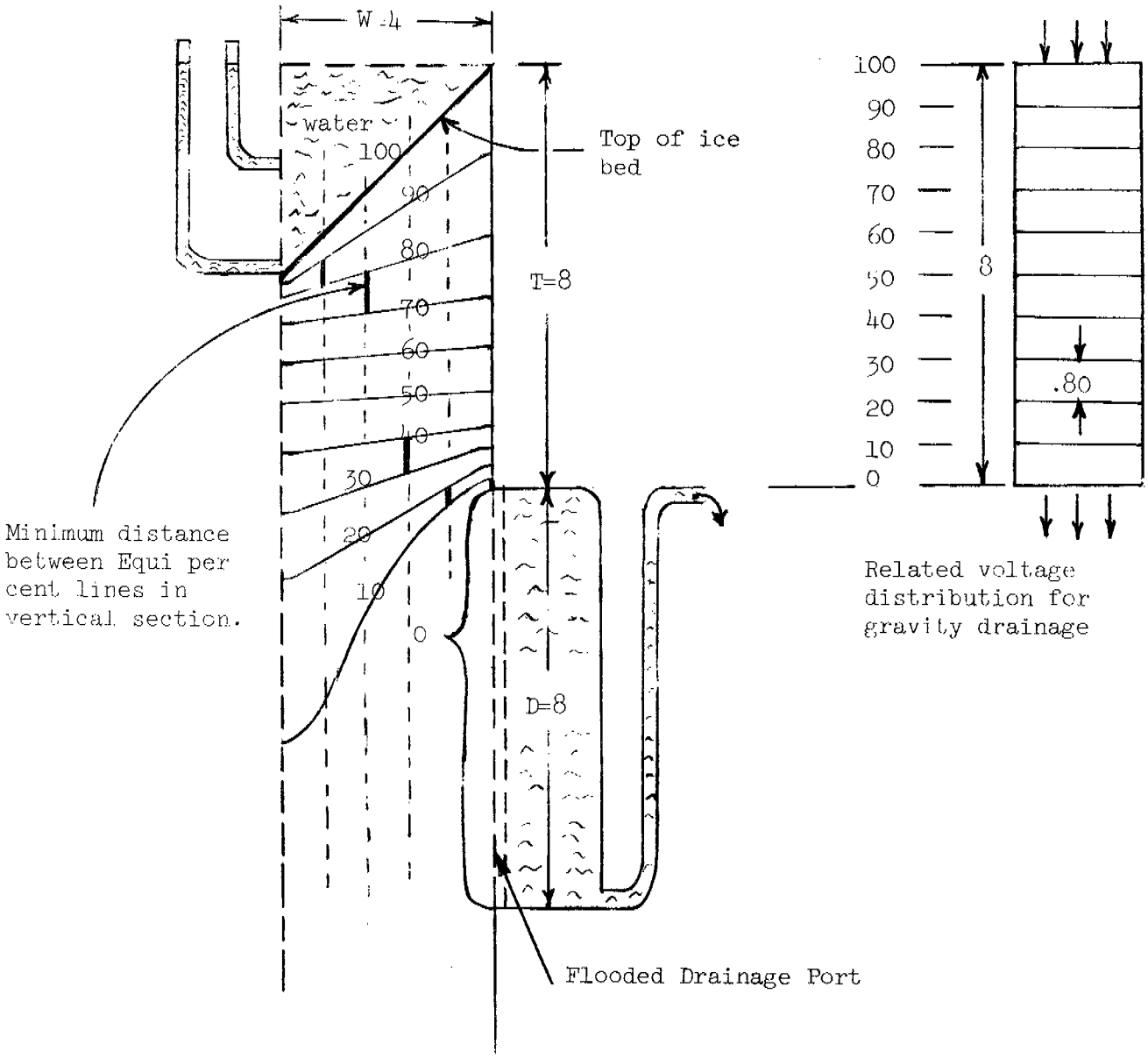

which is a minimum. This represents the position on that vertical section-line for which the vertical slip, $-v_z$, is a maximum. The ice rate, for perfect washing, cannot be allowed to exceed the maximum $-v_z$ of any vertical section.

Thus

$$v_{i\ max} = (-v_{z\ max})_{min}$$

where

$v_{i\ max}$ = maximum theoretical ice rate on relative basis from the analog

$(-v_{z\ max})$ = maximum vertical slip rate for any vertical section, same basis

$(-v_{z\ max})_{min}$ = minimum of all the maximum vertical slip rates measured, same basis.

Thus

$$V_{i\ max} = \frac{v_{i\ max}}{-v_g}$$

where

$-v_g$ = the gravity slip rate on the same measurement basis as $v_{i\ max}$.

However, for engineering and operating reasons the v_i in this report will be taken as $0.95\ v_{i\ max}$ to insure a positive downflow of wash water. The V_i values reported in the analyses are thus

$$V_i = 0.95\ V_{i\ max} = \frac{0.95\ v_{i\ max}}{-v_g}$$

and, since by definition

$$v_i = 0.95\ v_{i\ max}$$

then

$$V_i = \frac{v_i}{-v_g}$$

It is important not only to achieve a satisfactory V_i, but also there must not be an excessive loss of wash water. The overall average net

downflow rate of wash water can be established by integrating the downflow rate (to the observer) over any horizontal cross section in the upper column or

$$(-v_w)_{ave} = \frac{1}{W}\int_0^W \left[(-v_z) - (v_i)\right] dW$$

which may frequently be simplified to

$$(-v_w)_{ave} = \left[(-v_z) - (v_i)\right]_{ave}$$

where

W = Width of half-column

$(-v_w)_{ave}$ = the average net downflow rate of wash water on same basis as $v_{i\ max}$ above.

When the constant potential lines are curved, it is easier to consider one of the constant potential lines in the upper section of the column as a measurement barrier. The total flow across this barrier (measured in the direction perpendicular to the barrier at any point) represents the total downflow (in the upper part of the column) relative to the bed. The actual or net downflow (seen by the observer) is the total downflow minus the water carried up by the moving bed. The vertical section-lines and two constant potential lines which are essentially equidistant make a convenient zone to carry out a stepwise integration. Thus, in consistent measurements and allowing for porosity, the net downflow divided by the total ice production gives the fraction of total ice produced which is consumed for washing. Thus

$$\text{Total Net Downflow} = (e)\sum_1^n \left[(-v_r)\, s_{pot} - v_i\, s_{hor}\right]$$

where

$-v_r$ = vector flow rate of liquid perpendicular to selected constant potential line and relative to bed, same basis as v_i.

s_{pot} = length of segment of potential line between two vertical section lines.

s_{hor} = horizontal distance between the equidistant, vertical section lines.

n = number of sections

Total ice production = $(1-e) \cdot v_i \cdot n \cdot s_{hor}$

Although the scalar measurements are the choice of the designer the only requirement is to make consistent measurements. Then the ratio

$$\frac{\text{Total Net Downflow}}{\text{Total Ice Production}} = \text{Fraction Net Wash} = \frac{\sum_{1}^{n} \left[(-v_r)s_{pot} - v_i s_{hor}\right]}{v_i \cdot n \cdot s_{hor}} \cdot \frac{e}{(1-e)}$$

and

Per Cent Net Wash = 100 X Fraction Net Wash

In the analyses in this report e is taken as 0.5 and, therefore, $\frac{e}{1-e} = 1$.

Another important quantity to know is the brine rate. Assume that 100 lbs of slurry from the freezer consists of 25 lbs ice and 75 lbs brine. Assume also that the total conversion of sea water feed is to be 40% ice and 60% waste brine. The amount of brine reject is $25 \times \frac{60}{40} = 37.5$ lbs. The amount of brine returned to the crystallizer is 75 - 37.5 = 37.5 lbs. If the waste brine is tapped from the bottom of the column and <u>if</u> only the recycle were desired to go up with the ice, the desired ratio of brine to ice is $\frac{37.5}{25} = 1.5$.

The brine rate can be expressed as

$$(v_b)_{ave} = \left[(v_z) + (v_i)\right]_{ave}$$

where

$(v_b)_{ave}$ = the average net upflow rate of brine. See definition of $(-v_w)_{ave}$.

and a dimensionless brine rate

$$\frac{V_b}{V_i} = \frac{(v_b)_{ave}}{-v_i} \text{ at } V_i \text{ design}$$

The column geometry, of course, establishes the actual v_b, but columns of V_{b/V_i} of approximately 1.5 would be economical in

recirculation costs. At operating rates representing part load, the $\frac{V_b}{V_i}$ will increase (12). Thus the practical aspect of operating economy for a real process plant also suggests the desirability of a substantial bed length below the drainage port. However, the overall process must be considered in order to establish the preferred brine leakage in a given instance.

It must be stressed that the vector, $-v_g$, as used in making the analysis has meaning only in its simultaneous use with construction vector, v_i; and both v_i and $-v_g$ must refer to the same measurement standard.[1] Subsequent application of the results to a real column is perfectly straightforward in that

$$\left(\frac{v_i}{-v_g}\right)_{\text{analysis}} = V_i = \left(\frac{v_i}{-v_g}\right)_{\text{real}}$$

and V_i remains the basic criterion of thruput qualities of the column. To predict the real lineal ice rate one can expect from a column it is necessary to know the real value of $-v_g$ for a specific bed as discussed in the previous section.

To illustrate further the construction basis for v_i and v_g, Figure 6 shows a column in which the drainage area outside the column is open, again with the pressure at the outlet being the same as that over the column. It is easily seen that the operating Vi for the flooded drainage port, as in Figure 5, is adjustable downward from the design maximum to essentially zero by the simple expedient of increasing the back pressure. In the diagram representation this would be indicated by raising the outlet position of the outlet pipe. It is interesting to note that the same Teledeltos analog is used, and the same construction v_i is obtained. However, the potential difference is represented by a shorter head of liquid; the related uniform total voltage distribution for gravity drainage is represented by this shorter distance; the distance between equi-per cent lines is shorter; and the construction v_g based on the reciprocal distance is greater. This, of course, has nothing to do with the real v_g which would probably be little affected (for identical crystals) by changes in thruput.

Figure 7 is a diagram to represent a pressurized column. The pressure above the column is represented by an equivalent column of water. The voltage distribution for representation of v_g is now spread over a much greater height. In other words the crystal bed which would exactly consume all of the gravity head available

FIGURE 6

ANALYSIS OF ANALOG

Representation of Voltage Increments to Establish Relative $-v_g$ and $v_{i\ max}$

Pressure Along Open Drainage Port = Pressure Above Column

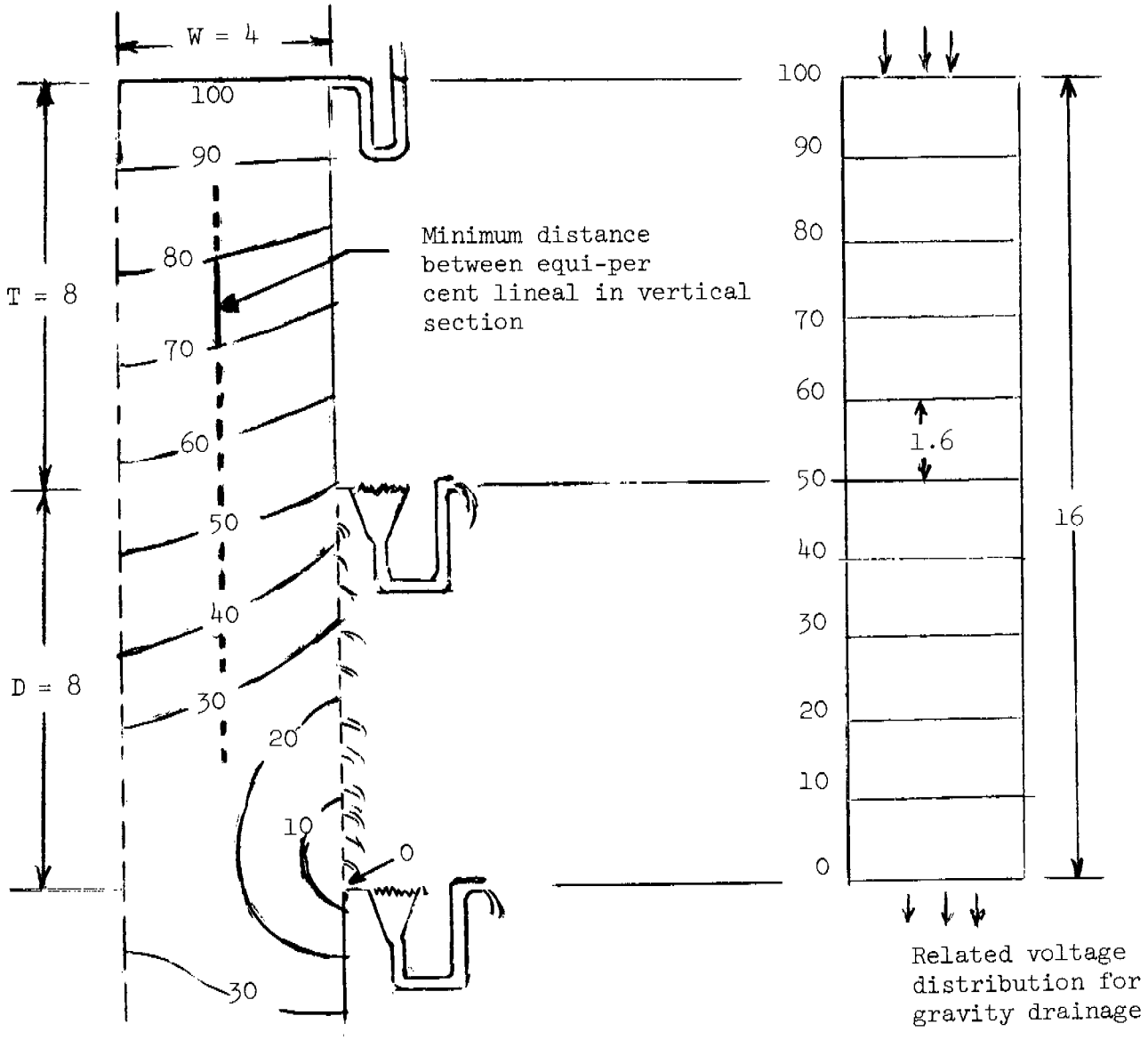

FIGURE 7

ANALYSIS OF ANALOG

Representation of Voltage Increments to Establish Relative $-v_g$ and $v_{i\ max}$

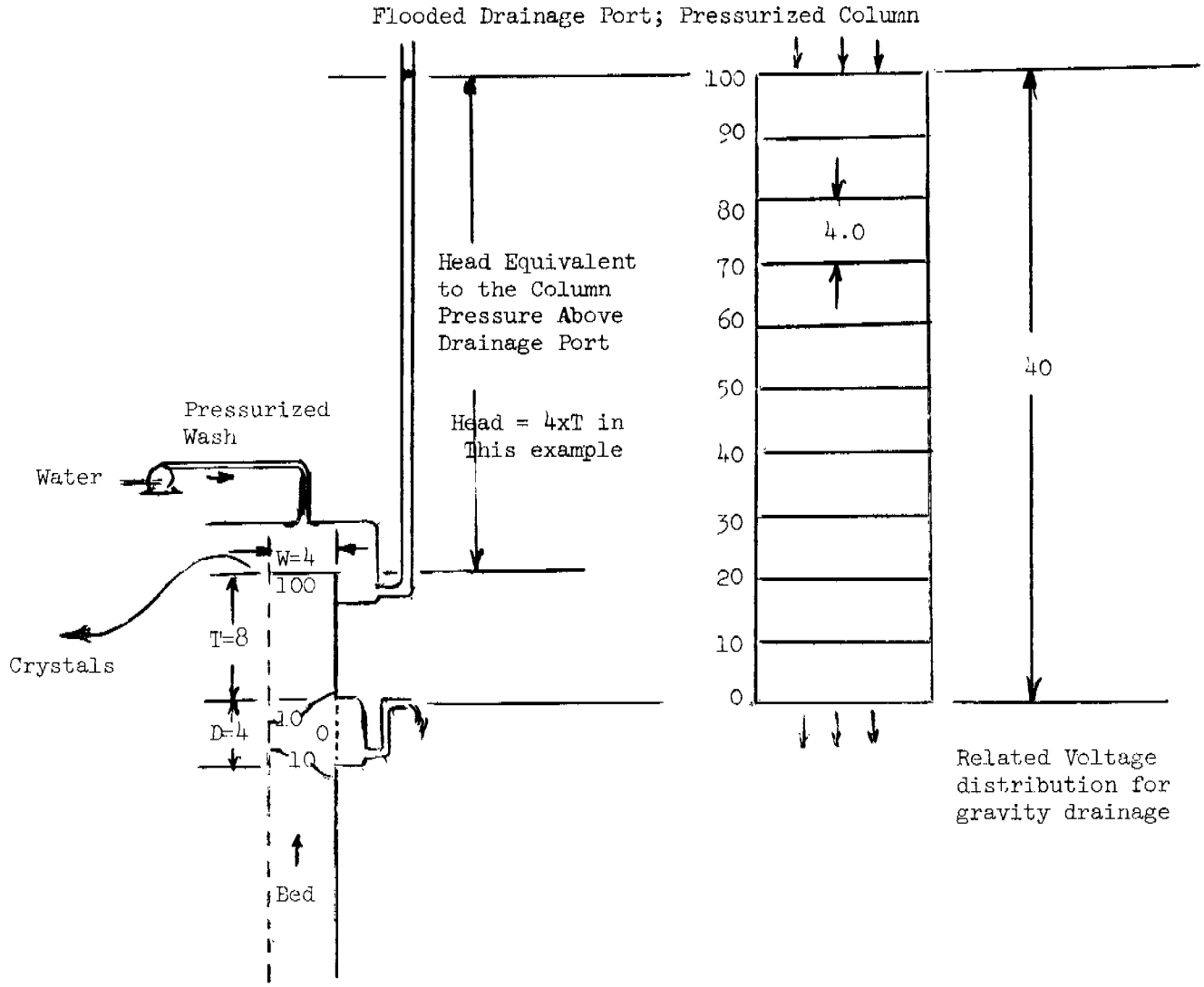

is equal to the head of liquid between the outlet and the representative liquid level above the column.

Because the equidistant potential lines for this liquid head are now widely spaced, the construction v_g based on the reciprocal distance is small. Thus $(v_i/-v_g)_{analysis}$ or V_i will be large.

This analog method should not be construed as an endorsement for any conceptual geometry which yields an analysis which shows a very high V_i. The delicate balance of pressures to control the movement of the almost-free piston poses an engineering problem of controlled bed movement which is not faced when the hydraulic forces are small. The possibility of breakthrough at the drainage port or plugging of drainage screens is not recognized in the analysis.

ESTABLISHING THE BRINE CROWN

Having established the V_i, the V_b/V_i, and the per cent net wash, the principal remaining item of information pertaining to the hydraulics of the piston-bed operation is the location of the zone of demarcation between the wash water and the brine. This can be done in three different ways.

Method 1.

Similar to the example vectors in Figure 3, many resultant (or streamline) vectors can be entered on an analog diagram by geometric construction. The flow vectors relative to the bed will be perpendicular to the constant potential lines and proportional to the inverse of their spacing. To this can be added the vertical ice-vector which the designer must choose since the water is carried bodily with the ice. The resultant vectors represent the magnitude and direction of flow of water or brine in the moving column as seen by an outside observer. Brine and water flow lines can be drawn from these vectors and the interface between the brine and water flow lines represents the location of the brine crown.

Method 2.

The prinicipal objection to Method 1 is that it is extremely tedious. Furthermore, the information of greatest importance is the location of the peak of the brine crown insofar as the margin of safety in avoiding a brine breakthrough in the operation of an actual column is largely indicated by the location of this peak.

It is very easy to determine the locus of points in the moving bed where the flow is horizontal to the observer. The points desired are those for which the vertical downward flow vector between constant-potential lines exactly equals the vector for ice movement, or where $(-v_z) = v_i$. The vector distance v_i is based on the standard already described and where h is the vertical distance between constant potential lines. A pair of dividers can be set to the distance $\frac{1}{v_i}$. Between any two constant-potential lines there will be a location where the vertical distance between these lines exactly equals this construction $\frac{1}{v_i}$. Here $(-v_z) = v_i$ and the only flow, to the observer, is horizontal. Mid-points of these vertical segments between constant potential lines can be quickly located starting near the drainage port and proceeding toward the center line (the side opposite the drainage port of the half-column, as drawn) progressively for each upward increment of potential. A line drawn through these mid-points

leads to the brine peak at the center line. For the point on the center line, the horizontal component also is zero. This point, which in theory has neither vertical nor horizontal component, is unique. The downward-sloping locus (downward in the direction away from the center line and toward the drainage port) represents a locus of horizontal brine-flow. The complete brine-crown can be reasonably drawn by inspection since it connects definite points that can be established on the center line and, in principle, at the drainage port by this method of construction. However, crowding of potential lines makes the exact location of the points near the drainage port difficult to locate. These points are not crucial to the evaluation.

It is possible, with more complex washing geometries, for this locus actually to show a reverse curvature and pass through a maximum between the drainage wall and the center line. Physically this means that on the upward (or positive) slope away from the center line the horizontal component represents a horizontal sweep of wash-water toward the drainage port. The prediction of the overall shape of this brine crown by inspection is less evident than it is when the locus has no inflection. The point at which the brine-water interface cuts the negative slope must be found by Method 1 or the method which is next described. However, the mid-point locus method with the center-line intersection still serves to characterize the quality of the column geometry being inspected. Because of the ease and definitive significance of Method 2, it serves as the principal method for analysis of the designs to be presented.

Method 3.

It is also possible by changing the boundary conditions to incorporate the ice velocity and thereby to determine directly the constant voltage lines normal to the flow lines for the moving bed as seen by an observer. This is done by modifing the previous equations as follows:

$$v'_z = -K \frac{\partial}{\partial z} \left[P + \rho \frac{g}{g_c} z \right] + v_i$$

$$v_x = v'_x = -K \frac{\partial}{\partial x} \left[P + \rho \frac{g}{g_c} z \right]$$

where

v' = velocity as seen by observer, ft/min

For gravity flow P is constant and

$$v_g = -K \frac{\partial}{\partial z} \left[P_{\text{constant}} + \rho \frac{g}{g_c} z \right]$$

$$= -K \frac{\partial}{\partial z}\left(\rho \frac{g}{g_c} z\right)$$

$$= -K \rho \frac{g}{g_c}$$

By definition

$$\frac{v_{ice}}{-v_g} = V_i$$

and $$v_{ice} = V_i \left(K \rho \frac{g}{g_c}\right)$$

Substituting

$$v'z = -K \frac{\partial}{\partial z} \left[P + \rho \frac{g}{g_c} z\right] + V_i K \rho \frac{g}{g_c}$$

$$= -K \frac{\partial}{\partial z} \left[P + \rho \frac{g}{g_c} z - V_i \frac{K}{K} \rho \frac{g}{g_c} z\right]$$

$$= -K \frac{\partial}{\partial z} \left[P + (1 - V_i) \rho \frac{g}{g_c} z\right]$$

and

$$v_x = -K \frac{\partial}{\partial x} \left[P + (1 - V_i) \rho \frac{g}{g_c} z\right]$$

or

$$\phi' = \left[P + (1 - V_i) \rho \frac{g}{g_c} z\right]$$

With these boundary conditions one obtains a series of constant-voltage contour lines. The flow lines for water and brine are the lines of steepest ascent or, essentially, the normals; and the brine crown is seen directly. It is necessary as in Method 1, to supply a value for V_i; and this must be determined from the stationary-bed analog.

Also the constant-voltage lines most important to the analysis are crowded into a small fraction of the total applied voltage; and the high sensitivity required adds greatly to the effort required to produce this analog. The analyses by Method 3 were found to indicate almost the same brine peak as Method 2. Locating exactly all portions of the brine crown and projecting the streamlines is helpful in a descriptive way. For appraisal of a given design geometry Method 2, the mid-point locus method is sufficient.

Two examples are presented to show the use of Method 3. The boundary conditions for two geometries

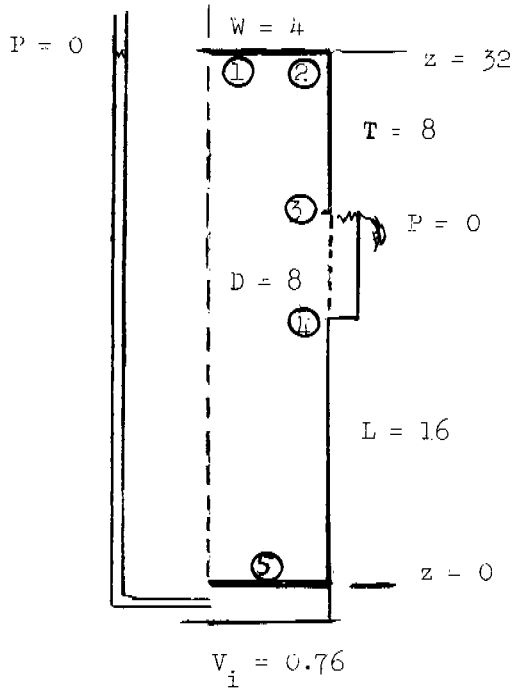

(See Analog I-A)

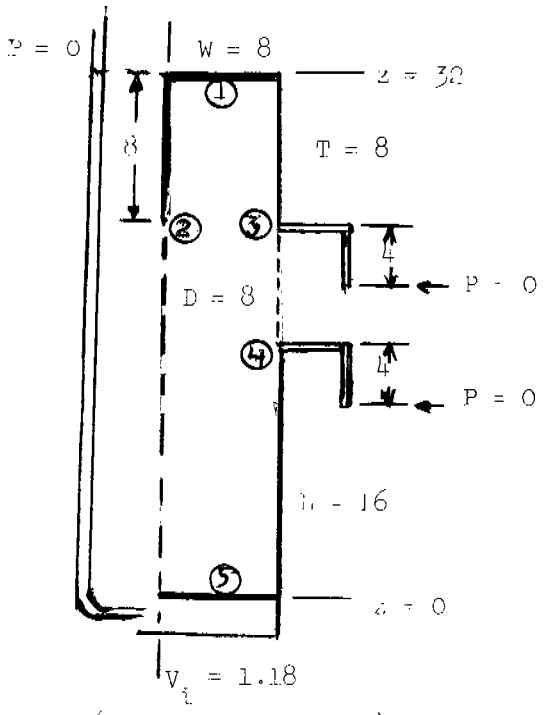

(See Analog XVI -A)

for which the V_i has been established by Method 2 are determined as follows

$$\phi_1' = P + (1 - V_i)\rho\frac{g}{g_c} z$$

$$= 0 + (0.24)\rho(32)$$

$$= 7.68\rho$$

$$\phi_2' = \phi_1'$$

$$\phi_3' = 0 + (0.24)\rho(24)$$

$$= 5.76\rho$$

$$\phi_4' = 8\rho + (0.24)\rho(16)$$

$$= 11.84\rho$$

$$\phi_5' = 32\rho$$

$$\phi_1' = 0 + (-0.18)\rho(32)$$

$$= -5.76\rho$$

$$\phi_2' = 8\rho + (-0.18)\rho(24)$$

$$= 3.68\rho$$

$$\phi_3' = -4\rho + (-0.18)\rho(24)$$

$$= -8.32\rho$$

$$\phi_4' = -4\rho + (-0.18)\rho(16)$$

$$= -6.88\rho$$

$$\phi_5' = 32\rho$$

If the lowest and highest potentials are now made to represent 0% and 100% of the applied voltage, the other potentials may be proportioned at their appropriate intermediate values. Thus

$\phi_1' = 7.32\%$	$\phi_1' = 6.36\%$
$\phi_2' = 7.32$	$\phi_2' = 29.8$
$\phi_3' = 0$	$\phi_3' = 0$
$\phi_4' = 23.15$	$\phi_4' = 3.57$
$\phi_5' = 100$	$\phi_5' = 100$

and the numerous linear intermediate values can be calculated by the same procedure between ϕ_1' and ϕ_2', as required in the second example, and between ϕ_3' and ϕ_4' for both the first and second examples.

DESIGN EXAMPLES

Eighteen examples of analyses by the electrical analog technique are presented in the subsequent diagrams. All of the examples are for rectangular columns and flooded beds. The diagrams are 1/4 scale reproductions of analog tracings.

The principle purpose in showing these designs is to introduce the method for a variety of columns and thereby to permit significant generalizations. Consequently, the geometric proportions for the present are simple whole-number ratios.

Although the thinking in these laboratories has been that the unit values of the numbers representing distances on the diagrams are feet, it should be noted that the analogs apply to any column of the identical geometry.

Design I, in Figure 8, represents a column with a deep lower bed and a wide drainage port. The operating conditions selected have the liquid pass through the drainage port into a liquid-filled chamber (i.e. a flooded drainage-port). The constant-voltage lines shown in Diagram I will be the same for the representation of any selected back-pressure on the outlet chamber; but for the specific condition of having the pressure outside the drainage wall at the top of the drainage port exactly equal to the pressure above the bed, the V_i is 0.76. For the geometry represented by Design I, when the V_i is 0.76 the V_b is 1.57 times V_i. It is interesting to note that even with a generously sized drainage port the V_i under the conditions imposed is considerably less than 1.0.

The V_i, can for operational purposes, be reduced to any desired value by simply increasing the back pressure outside the drainage port.

The V_b is primarily a function of the operating V_i and the bed geometry. It was pointed out earlier that this design approach would assume that resistance to bed movement (e.g. wall friction) would be met by making the real bed somewhat longer than is indicated by the analog. The feed pressure is accordingly increased such that V_b would in fact by the same value as for a frictionless bed. Thus, V_b is tied directly to V_i.

Diagram I-A is a streamline analog, made according to Method 3, of the same column as Design I. The brine crown is the line which divides the opposed streamlines. The locus of horizontal flows is also drawn through the horizontal tangents to the streamlines. This locus line, transferred

to Design I, permits comparison with the brine peak as determined by Method 2, the mid-point locus method. The latter method gives a location which is slightly high because the stepwise procedure for the mid-point locus method provides no basis for recognizing the curvature near the center line. However, all judgment values are derivable from Figure I by itself.

Design II is a column having the drainage port area sharply reduced from the column in Design I. The bed above and below the port is the same. The brine peak is considerably higher in Design II; and, more important, the V_i drops to 0.56 because of the crowding from all of the liquid trying to squeeze through a smaller and smaller flow path as it nears the outlet. The V_b/V_i remains about the same as for Design I.

Design III is Design II inverted. Here there is a much longer drainage height above the port, but the lower bed has been shortened. The results are interesting. The V_i has increased from the 0.56 of Design II only to 0.59. This demonstrates conclusively the importance, as many have long suspected, of having an adequate drainage area. Although there is, in this case, little improvement for V_i, the V_b for the shortened lower bed jumps from 1.53 V_i in Design II to 3.07 V_i in Design III.

Design IV, in Figure 9, is another example of a column with its drainage port positioned toward the lower end of the column. Compared with the previous columns, this column is somewhat wider, and its drainage port is one-half the height of that in Design I.

There has been much conjecture about the effective contour of the bottom of the bed. The normal sequence of the lower constant-pressure lines is gradually to spread apart as one proceeds up the center line. By trial and error the bottom 100% line was established such that the probe-tested 90% line did not diverge and, in fact, marginally converged toward the 100% line. Further exploratory probing (not shown in the diagram) revealed that rather severe arbitrary adjustments of the base line would have almost no influence on the upper bed and at most would merely have a minor effect on V_b. The question of bottom contour was checked once again, as shown in a subsequent design on a wider column; and it is concluded that the effect is too trivial to warrant further concern. All designs except Design III and Design XII are simply made with the base horizontal. It seems reasonable that a generally balanced slurry distribution would give a satisfactory mechanical performance for any column having a lower bed deep enough to develop a well-structured piston prior to the level of the drainage port. Minor imbalances would correct in the direction of a flat bottom by small local variations in V_b and by the redistribution of crystals during the compaction period.

Although Design IV is intended to represent approximately the design

FIGURE 8

Horizontal Top; Flooded Drainage Port; Pressure at Top of Drainage Port = Pressure above Column

Design	W	T	D	L	V_i	V_b	Net Wash (e=0.5)
I	4	8	8	16	0.76	$1.57V_i$	5.0%
I-A	Streamline Analog of Design I						
II	4	8	0.5	16	0.56	$1.53V_i$	5.0%
III	4	16	0.5	8	0.59	$3.07V_i$	5.0%

---------- Brine Crown

...o...o...o...o...o...o.. Mid-Point Locus Method for Projecting to Brine Peak at Center Line

——— . ——— . ———. —— Horizontal-Flow Locus as Established From Design I-A

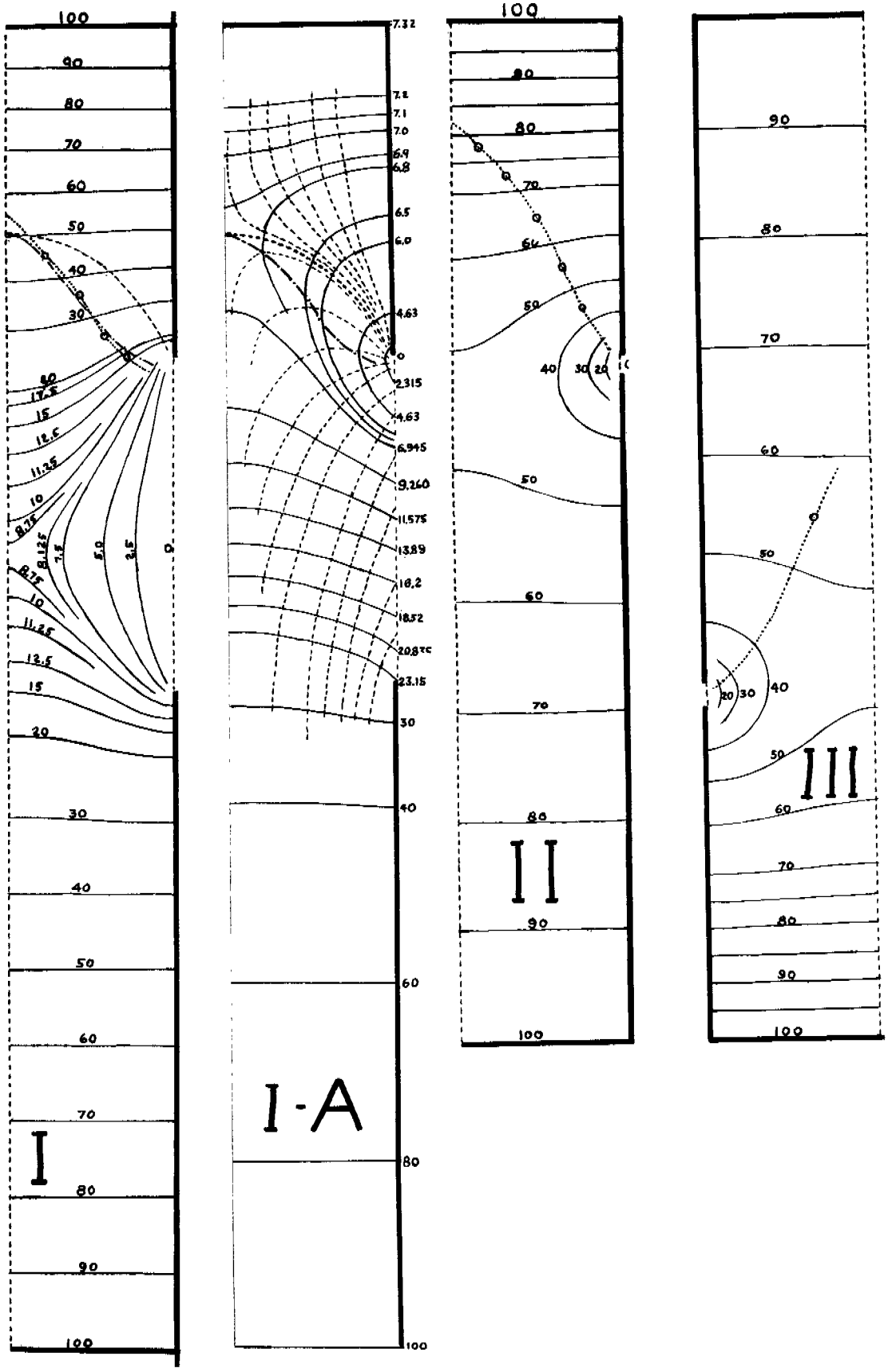
I
I-A
II
III

FIGURE 9

Flooded Drainage Port; Pressure at Top of Drainage Port = Pressure above Column

Design	Top Surface	Depth of Cut	W	T	D	L	V_i	V_b	Net Wash (e=0.5)
IV	Horizontal	0	6	16	4	6	0.65	$2.29V_i$	5.0%
I (Fig. 8)	Horizontal	0	4	8	8	16	0.76	$1.57V_i$	5.0%
V	V Cut	1	4	8	8	16	0.82	$1.55V_i$	5.04%
VI	V Cut	4	4	8	8	16	0.99	$1.43V_i$	5.10%

...Δ...Δ...Δ...Δ...Δ...Δ... Mid-Point Locus for Approximate Upper Boundary of Washing Zone

...o...o...o...o...o...o... Mid-Point Locus Method for Projecting to Brine Peak at Center Line

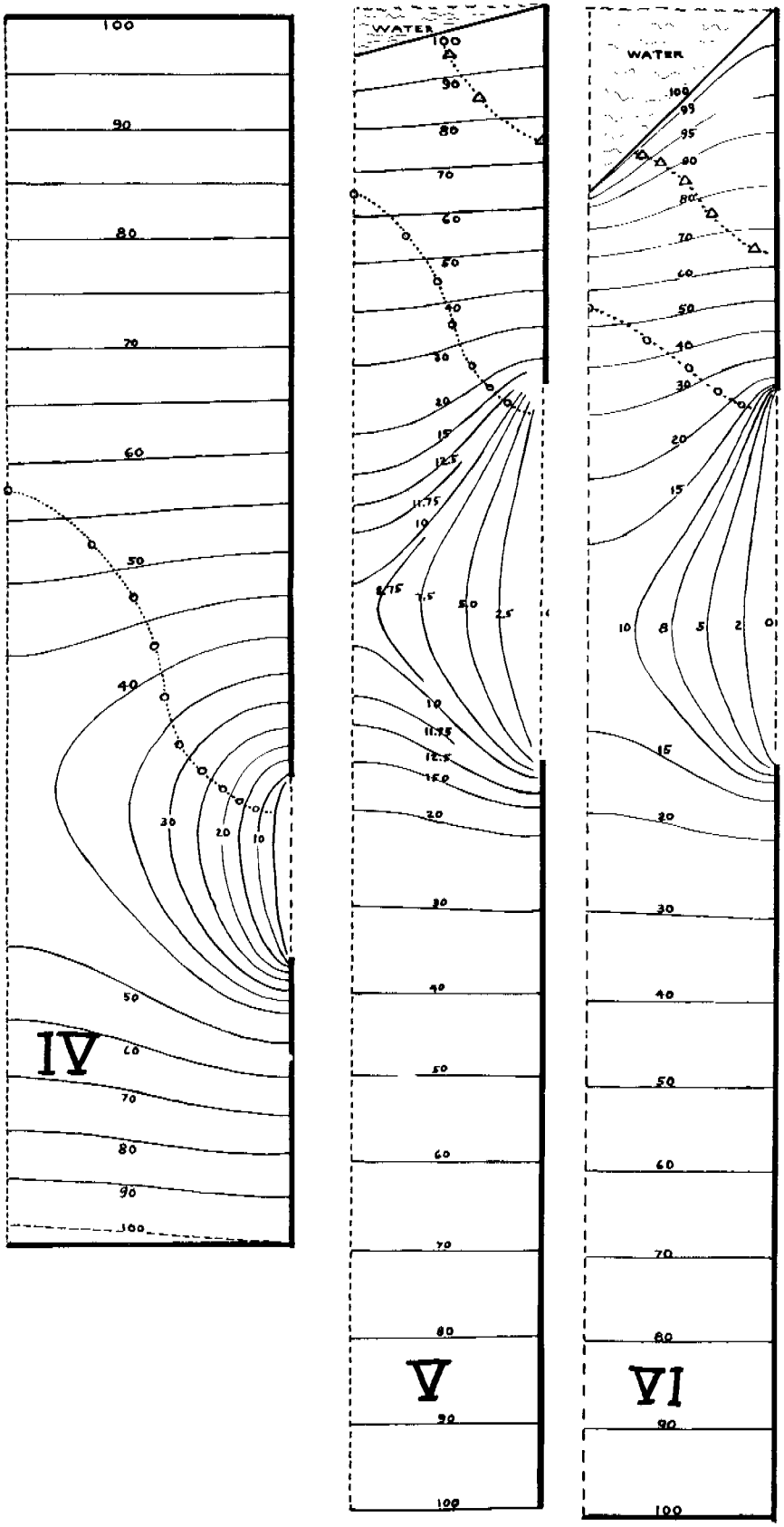
WATER
WATER
IV
V
VI

proposed by Johnson et.al., (6) for a circular column, no final interpretations should be made until an analog technique for a circular column has been established. For the design as shown, however, the V_i is 0.65 and the V_b is quite high at 2.29 times V_i. This analysis is also for a flooded bed, and the V_i for a drained bed would even be somewhat lower. If pilot plant studies were to indicate an operating V_i greater than predicted by this design method the explanation is most likely to be found either in the existence of channels or zones of high permeability which favor liquid flow or the formation of a more permeable real bed than is indicated by a measured permeability of a test bed prepared from a sample of the feed slurry. The position of the brine peak indicated in Design IV is far from the top of the column, and with operation considerably less than ideal one would still expect this column to produce specification water. This conservative design also suggests that the design standard adopted (i.e. $v_i = 0.95\ (-v_{i\ max})$) could have been modified in the direction of a smaller consumption of wash water.

Design V introduces for the first time the concept of a contoured top surface. The presence of a V-shaped cap of water at the top results in a positive hydraulic pressure which contributes to the wash-water flow-rate. An increase of V_i from 0.76 to 0.82 is observed in comparing Design I, which has a horizontal top-surface, with Design V in which the slope of the top surface is 1 in 4 from the center line to the column wall. Design V also introduces for the first time the hydraulic situation whereby there is actually an upflow (to the observer) of wash water in that part of the column least subjected to the hydraulic pressure resulting from the water layer in the V-cut. The two mid-point locus lines depicted in the diagram for Design V approximately bound the effective washing zone for the column. Brine reaches its maximum elevation at the brine peak. An upper boundary of a washing zone exists where there no longer exists a net downward component of wash water.

Design VI is a column having a 45° V-cut to the center line. The allowable V_i of 0.99 is a considerable increase which results from the hydraulic-pressure contribution of a deeper pool of water. The slope of the constant-pressure lines is reflected by a slight increase of wash-water loss over that for Designs I, II, III, and IV for which essentially horizontal lines are present in some portion of the washing zone. The design diagram indicates also that wash water enters only about 25% of the central top surface of this bed. The water which enters the remainder of the bed also is the source of the water which circulates into the upflow zones where it is carried out again.

Design VI is of interest in that it achieves the V_i which had originally (12) been expected for a draining-bed design.

The next logical progressive step to take after providing adequate drainage-port area is to permit the liquid to trickle directly through the drainage port into a vapor space. This is particulary of help in easing the exit flow of the upcoming brine. The analog apparatus was set up as shown in Figure 4 and the analysis $-v_g$ established as indicated in Figure 6. In Figure 10 are shown three columns of the same basic dimensions as Design I.

Design VII, in Figure 10, has a horizontal top. It is a very conservative design in that the upper column is quite long and is totally free of designed hydraulic disturbances. This again results in an almost negligible difference in downflow rate of wash water over the entire column near the top of the column. Because of the unflooded, or open, drainage port the brine peak is even lower than the peak in Design I, but the V_i of 0.95 is substantially greater than 0.76. The operation with an unflooded drainage port contributes about equally with the V-cut when comparing the V_i values of Designs I, VI, and VII. The reduction of back pressure on the drainage port, however, also makes it easier for the brine to flow upward and the V_b for Design VII is 1.83 V_i as compared to 1.43 V_i for Design VI.

Designs VIII and IX are perhaps the two most instructive designs in this report. Either introducing a 45° V-cut or cutting a center slot to the same depth as the bottom of the V gives, for a column of the proportions indicated, almost the same operating and washing performance. The V_i of 1.23 is approaching an ice rate which is twice that which would now be expected from a column as originally suggested (12) from these laboratories, but there are no significant changes in detail or operating principles.

The center-slot arrangement is particulary adaptable to an annulus column with a center-dump melter and is in accordance with the scale-up concepts which have been endorsed for several years by these laboratories. Overall considerations which include interrelation with other parts of the freezing process such as recycle, conversion, heat exchange, bulk melting of a bed not tightly packed (as proposed in 1960), crystallization procedures, and low-cost sources of shaft energy (including a butane Carnot cycle to replace a steam surface condenser) are beyond the scope of this report; but it is necessary to recognize that these interactions ultimately must be recognized. The first requirement, as is the case for preparing these preliminary column designs, is to have adequate design knowledge to permit the subsequent optimization as a routine procedure.

The scale-up of Design IX seems practical. The effective washing zone is a slightly more narrow band than it is in Design VIII, but it appears to be more than adequate for safe operation under expected

FIGURE 10

Open Drainage Port; Pressure along Drainage Port = Pressure above Column

Design	Top Surface	Depth of Cut	W	T	D	L	V_i	V_b	Net Wash (c=0.5)
VII	Horizontal	0	4	8	8	16	0.95	$1.83V_i$	5.0%
VIII	V	4	4	8	8	16	1.23	$1.62V_i$	5.07%
IX	Center Slot	4	4	8	8	16	1.22	$1.64V_i$	5.08%

...Δ...Δ...Δ...Δ...Δ...Δ... Mid-Point Locus for Approximate Upper Boundary of Washing Zone

...o...o...o...o...o...o... Mid-Point Locus Method for Projecting to Brine Peak at Center Line

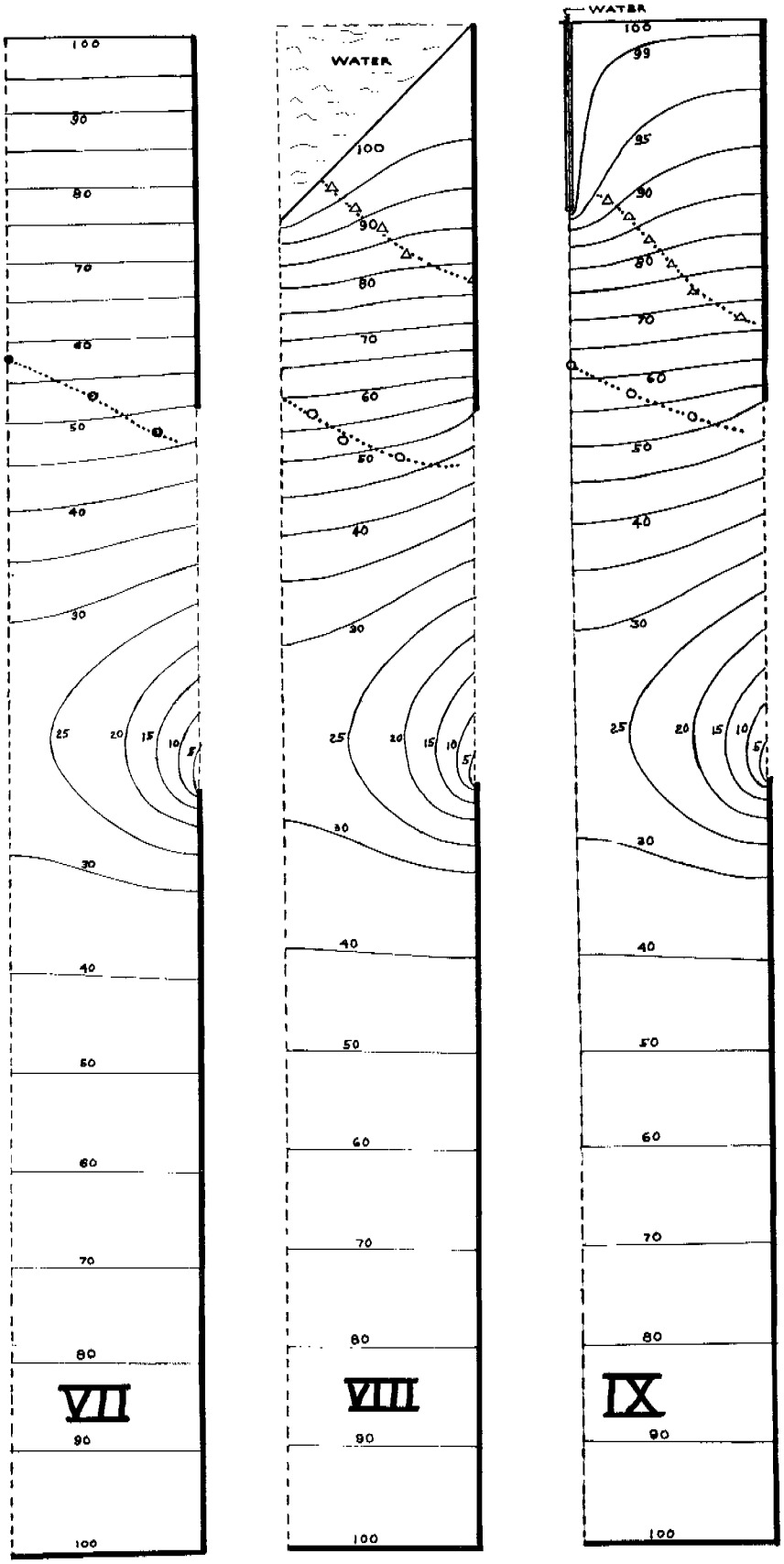
WATER
WATER
100
90
80
70
60
50
40
30
25
20
15
10
5
VII
VIII
IX

FIGURE 11

V-Cut Top; Open Drainage Port; Pressure along Drainage Port = Pressure above Column

Design	Depth of Cut	W	T	D	L	V_i	V_b	Net Wash (e=0.5)
VIII (Fig. 10)	4	4	8	8	16	1.23	$1.62V_i$	5.07%
X	4	6	8	8	16	1.11	$1.62V_i$	6.3%
XI	4	8	8	8	16	0.96	$1.62V_i$	9.9%

...Δ...Δ...Δ...Δ...Δ...Δ... Mid-Point Locus for Approximating Upper Boundary of Wash Zone

...o...o...o...o...o...o... Mid-Point Locus Method for Projecting to Brine Peak at Center Line

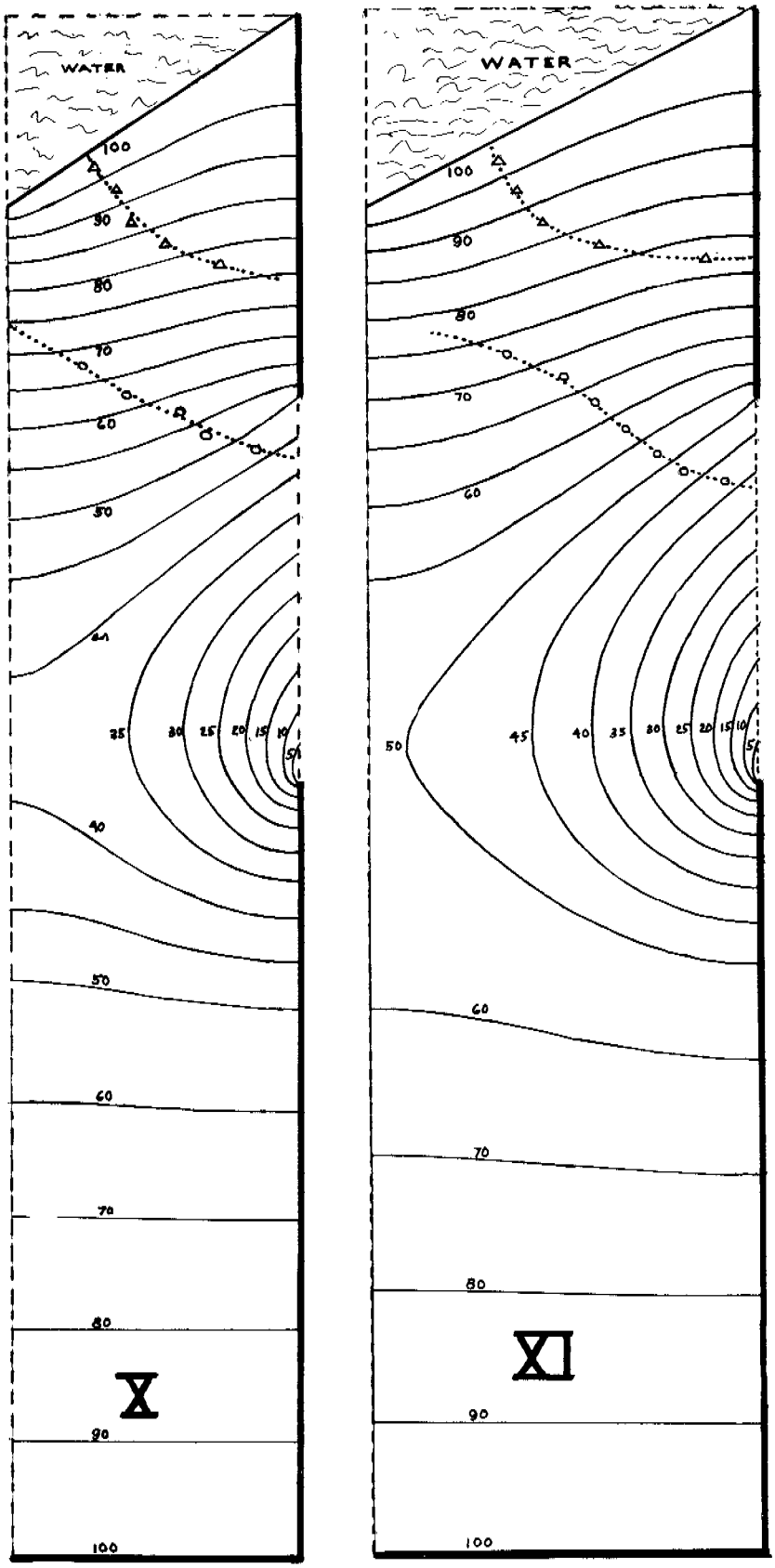
WATER
100
90
80
70
60
50
45
40
35
30
25
20
15
10
5
X
WATER
100
90
80
70
60
50
45
40
35
30
25
20
15
10
5
XI

conditions of plant operating fluctuations. For a $-v_g$ of 0.79 ft/min (Table 1) and a porosity of 0.5 the production rate from each square foot of column cross-section would be 1820 lbs. of final product water per hour. A horizontal-cutter blade which transfers pieces of porous ice to the center melter would represent no change from the present cutting method, although a slow moving blade is recommended in order that the ice pieces are sufficiently large to give a melting bed which retains an open structure during the melting operation.

A curved plate (shaped to the annulus curvature) with a cutting tip could project downward from the major cutter and thereby maintain the slot. Wash water is supplied merely by keeping the center slot filled.

Little has been done with design variations to explore the possibility of running the center slot somewhat less than full and thereby partially draining the ice by leakage of wash water back into the center slot. However, Design IX, as one or as concentric annuli, is sufficiently indicative of favorable operation to warrant future reference to it.

In Figure 11 are two V-cut designs which have the same depth of cut as Design VIII, the only difference being greater column width. Two comparative deficiencies appear for these designs: the V_i for Design X is 1.11 and for Design XI it is 0.96. In addition, the wash water loss is becoming more significant as the constant-pressure lines no longer fan into an essentially horizontal position in the active washing zone. In other respects, however, the column suggests functional operability.

For Designs XII and XIII, in Figure 12, a center-slot substitution for the V-cut was made for two different depths of the center-slot. Although the center-slot was found to function essentially as the equivalent of a V-cut in Designs VIII and IX, this is no longer true for the wider columns. Not only is there a substantial decrease in allowable V_i, but the proportion of the ice product lost to washing (24% for Design XIII) is unacceptable.

The assumption that the lower column can be properly represented by a horizontal base line was checked once again for a rather extreme test in Design XII. Even with the slight incline shown for the 100% line in Design XII there was some drift toward a true horizontal for the 95, 90, 85, and 80% lines before the lines began to diverge. A test with a more extremely inclined base line is not necessary. It would seem that a predetermined bottom-contour (such as an inverted -V cut, if desired) would have to be formed by mechanical means. For a lower bed of

substantial length a contoured bottom bed face would probably have little effect on the upper bed. Certainly the influence of the top contour on the lower bed is negligble for the designs in Figure 10.

An additional possible source of driving force for washing is to decrease the pressure in the open drainage-port to a value which is less than the gas pressure above the column. A practical difference in pressure to consider for the butane process is that which falls between the pressure of butane vapor in the melter and the pressure of butane in the freezer. In the remaining designs the difference in pressure is taken as that equivalent to the hydrostatic head of T/2. If the length T = 8 represents distance in feet, then the pressure differential is equal to 4 feet of water. This difference in pressure is allowable in the butane process without influencing the cost of compressing butane vapor. The pressure above the column is fixed by the pressure of butane for melting. The drainage-port chamber would have a vapor-line connection to the freezer. The vapor flow from this chamber to the freezer would be negligible and primarily for control of the desired back-pressure. General ice-formation in the drainage-port chamber is not possible at the designated pressure, but no claims are made regarding the upper section of the drainage port from which water of low brine content will emerge. This mode of operation should be subjected to a prolonged on-stream run at the pilot-plant level before final conclusions are drawn regarding operability.

The designs in the remaining three figures are all for columns having open drainage ports which are maintained at a gas pressure lower (by T/2) than the gas pressure above the column. The contributions from this added driving force are significant.

Design XIV, in Figure 13, is identical in all respects with Design VIII except for the drainage-port pressure. The result is a V_i of 1.83, the highest V_i of any design in this report. This represents a 50% increase in rate over Design VIII. For a $-v_g$ of 0.79 ft/min (Table I) and a porosity of 0.5 the production rate from each square foot of column cross-section would be 2700 lbs. of final product water per hour. The V_b for Design XIV is only 1.54 V_i and the wash water loss of 5.4% is only slightly above the design minimum. Most of the water which does the washing enters near the base of the V-cut as shown by the upper boundary of the wash zone. A center-slot analog for the same column dimensions was not prepared; but the great similarity between flow patterns in Designs VIII and XIV suggests that a comparable performance can be expected as was shown for the relationship between Designs VIII and IX.

The performance indicated for Design XV, which is geometrically identical to Design XII, is an improvement only in regard to the V_i,

FIGURE 12

Center Slot; Open Drainage Port; Pressure along Drainage Port = Pressure above Column

Design	Depth of Cut	W	T	D	L	V_i	V_b	Net Wash (e=0.5)
IX (Fig. 10)	4	4	8	8	16	1.22	$1.64V_i$	5.08%
XI (V-Cut Fig. 11)	4	8	8	8	16	0.96	$1.62V_i$	9.9%
XII	4	8	8	8	16	0.81	$1.76V_i$	12%
XIII	6	8	8	8	16	0.88	$1.71V_i$	24%

...Δ...Δ...Δ...Δ...Δ...Δ... Mid-Point Locus for Approximate Upper Boundary of Wash Zone

...o...o...o...o...o...o... Mid-Point Locus Method for Projecting to Brine Peak at Center Line

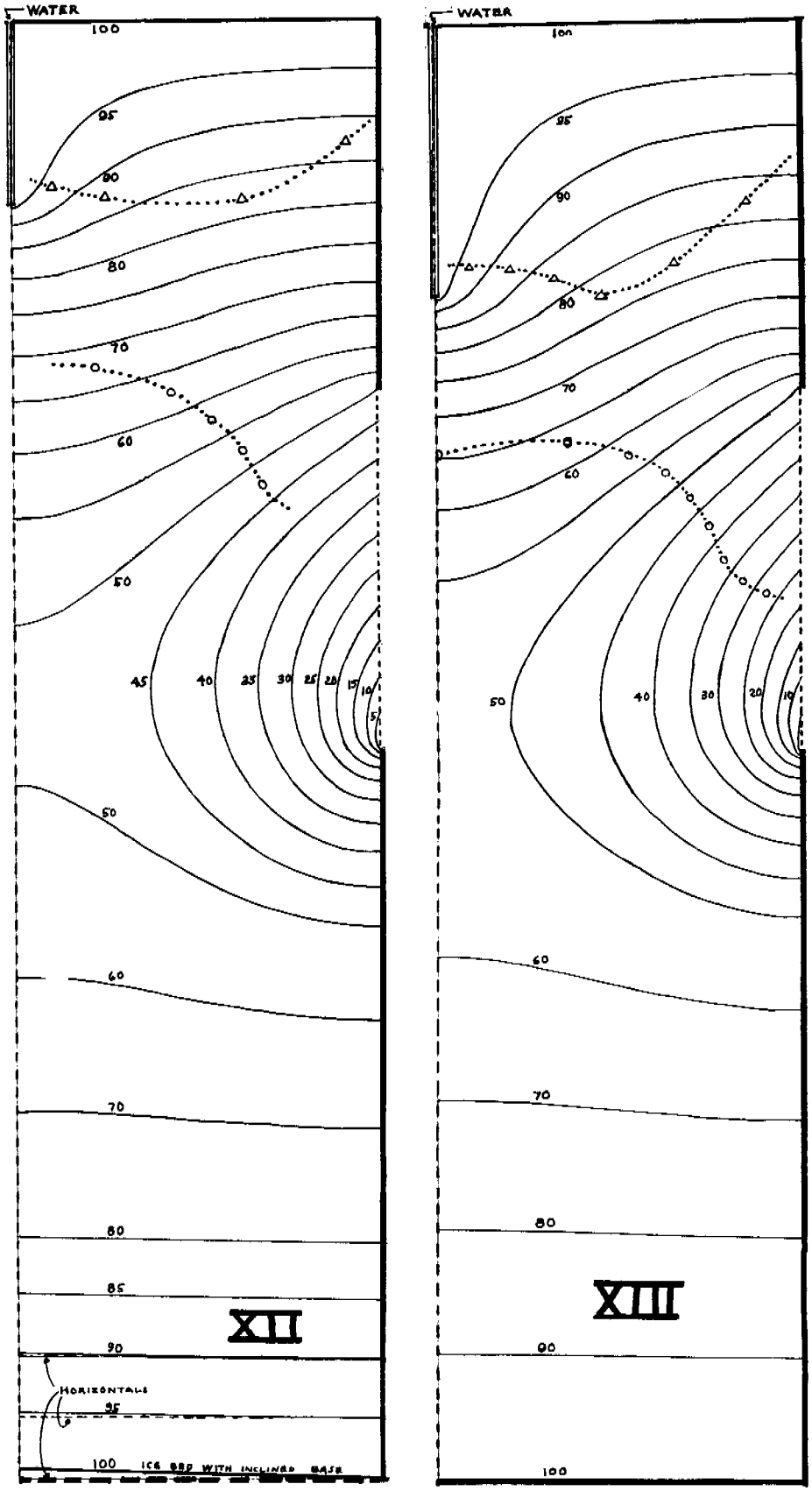
WATER
100
95
90
80
70
60
50
45
40
35
30
25
20
15
10
5
50
60
70
80
85
90
XII
HORIZONTALS
95
100
ICE BEP WITH INCLINED BASE
WATER
100
95
90
80
70
60
50
40
30
20
10
60
70
80
90
XIII
100

FIGURE 13

Open Drainage Port; Pressure along Drainage Port is Less than Pressure above Column by the Equivalent of a Hydrostatic Head T/2

Design	Top Surface	Depth of Cut	W	T	D	L	V_i	V_b	Net Wash (e=0.5)
VIII (Fig. 10)	V-Cut	4	4	8	8	16	1.23	$1.62V_i$	5.07%
XIV	V-Cut	4	4	8	8	16	1.83	$1.54V_i$	5.4%
XII[1] (Fig. 12)	Center Slot	4	8	8	8	16	0.81	$1.76V_i$	12%
XV	Center Slot	4	8	8	8	16	1.15	$1.75V_i$	13%

1 Pressure along Drainage Port = Pressure above Column

...Δ...Δ...Δ...Δ...Δ...Δ... Mid-Point Locus for Approximate Upper Boundary of Wash Zone

...o...o...o...o...o...o... Mid-Point Locus Method for Projecting to Brine Peak at Center Line

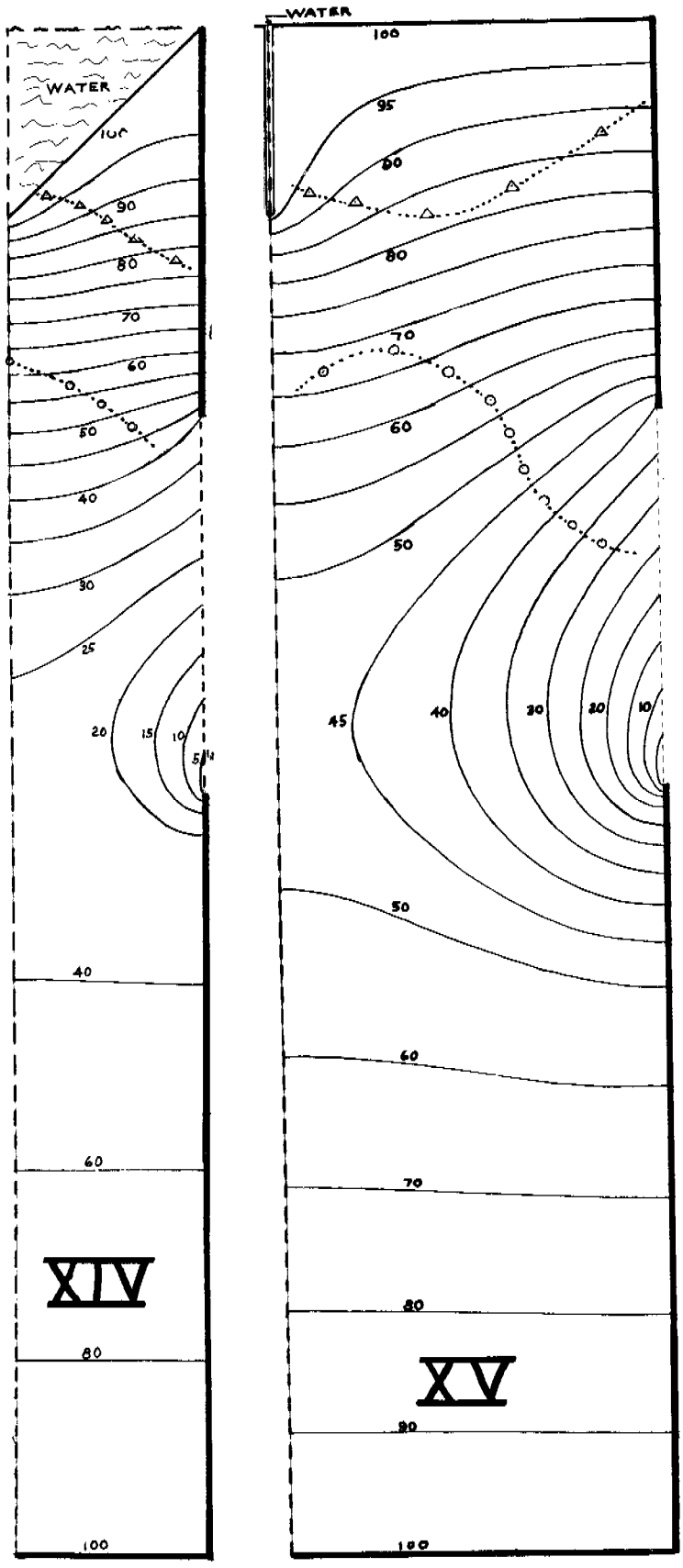
WATER
100
90
80
70
60
50
40
30
25
20
15
10
5
40
60
XIV
80
100
WATER
100
95
90
80
70
60
50
45
40
30
20
10
50
60
70
80
XV
90
100

1.15 as compared with 0.81. The wash water loss, 13% of the ice product, is not favorable. Primarily this shows the significance of increasing the column width and introducing no helping feature to compensate.

Design XVI in Figure 14 represents one effort to improve a wide column; and, in this instance, the center slot is extended to the same level as the top of the drainage port. Surprisingly this extension contributed almost nothing to the V_i, which is 1.18 for Design XVI and 1.15 for Design XV. The principal change results from the much greater horizontal sweep of wash water toward the drainage port with the result that 45% of the ice production is lost to washing.

Although this column represents a most unsatisfactory design, it provides an opportunity to make a severe test of the mid-point locus method to predict the brine peak and the upper boundary of the wash zone. Design XVI-A is the streamline analog of Design XVI.

The boundary voltages were set for the center slot as developed on page 31. For the open drainage-port the potential gradient is so small that it was set uniformly for 0 rather than over a gradient of 3.57% of the total. The approximation is justified because the steep voltage gradient near the base of the drainage port would have resulted in no observable difference in the streamlines.

The horizontal flow locus from the streamline analog checks the mid-point locus extremely well. Likewise the brine peak and the portion of the center slot which provides the wash water are both accurately predicted by the mid-point locus method in Design XVI. In this instance the deep center cut actually forces the brine peak to be a low point in the brine crown. Insofar as this column is not representative of a good design no effort will be made to resolve this special case of inappropriate terminology. It is of interest to note that the true wash zone as noted from the streamlines represents a somewhat more stable column operation than one would infer from the mid-point locus lines. But most significant is that this is an example of the design method for which the hydraulics of an intricate, complex, moving piston-bed resolve into a clearly discernible flow pattern.

The final two designs in Figure 15 of the report represent another effort to improve the performance of a wide column, this time by introducing more than one vertical slot. The complete annulus-column represented by Design XVII has three slots and that represented by Design XVIII has seven. Design XVII showed little improvement in V_i, but the product consumed for washing was reduced from 45% to 29%. Design XVIII has a remarkable V_i of 1.44 and the net wash has been

reduced to 12.5%. The increase in V_i results from the hydraulic pressure contribution across the bed. Multiple-slot beds might permit essentially the operation of a piston bed in a convenient manner and yet equal the hydraulic performance that would be attained by a bed which carries a column of wash water and must function in a complicated manner with a submerged cutter.

A characteristic feature of these multiple-slot beds is the existence of independent zones positioned between the slots where no washing takes place.

The eighteen designs in this report are not an exhaustive presentation of designs for rectangular columns. Some designs are obviously better than others and some are totally unacceptable. The easy interpretation of the analogs presented will hopefully contribute to a better understanding of existing piston beds and to improve conceptual designs.

In addition to the specific objective of setting forth a design method for piston-bed columns as used by various processes, there is in these laboratories a concurrent concern with many of the other engineering requirements for a large-scale freezing process using a low-cost secondary refrigerant. These include the freezing step, direct vaporizing-condensing heat-exchange (14), bulk-melting of open-structured beds (12), and the use of the freezing process to serve as a surface-condenser for low-pressure steam from a power plant (15). The selection of some of the design examples was influenced by an awareness of these related problems, but discussion of designs in this context goes beyond the scope or needs of this report. It is suggested, however, that appropriate and related experimental and design activity could beneficially be directed toward the several economically significant elements of a freezing process which uses an inexpensive secondary refrigerant.

ACKNOWLEDGEMENT

The authors gratefully acknowledge the assistance of S. H. De Young and S. G. Bolotin in applying the electrical analog technique, and the helpful suggestions from J. H. Pendergrass in developing the streamline analyses.

FIGURE 14

Open Drainage Port; Center Slot; Pressure along Drainage Port is less than Pressure above Column by the Equivalent of a Hydrostatic Head T/2

Design	Depth of Cut	W	T	D	L	V_i	V_b	Net Wash (e=0.5)
XV (Fig. 11)	4	8	8	8	16	1.15	$1.75V_i$	13%
XVI	8	8	8	8	16	1.18	$1.62V_i$	45%
XVI-A	Streamline Analog of Design XVI							

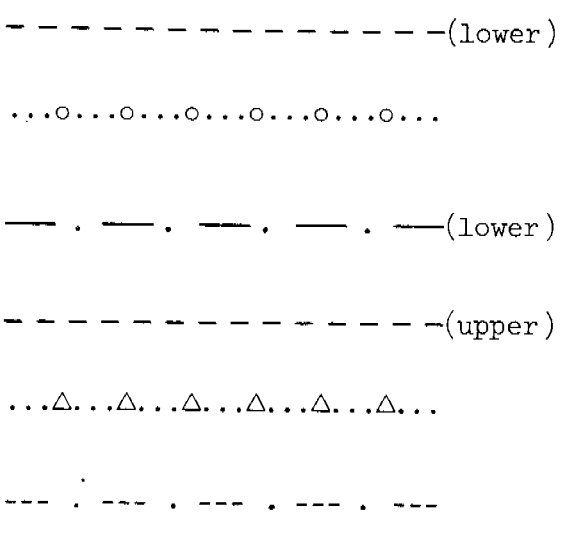

Brine Crown

Mid-Point Locus Method for Projecting to Brine Peak at Center Line

Horizontal-flow Locus as Established from Design XVI-A

True Upper Boundary of Washing Zone

Mid-Point Locus for Approximate Upper Boundary Washing Zone

Upper Horizontal-Flow Locus as Established from Design XVI-A

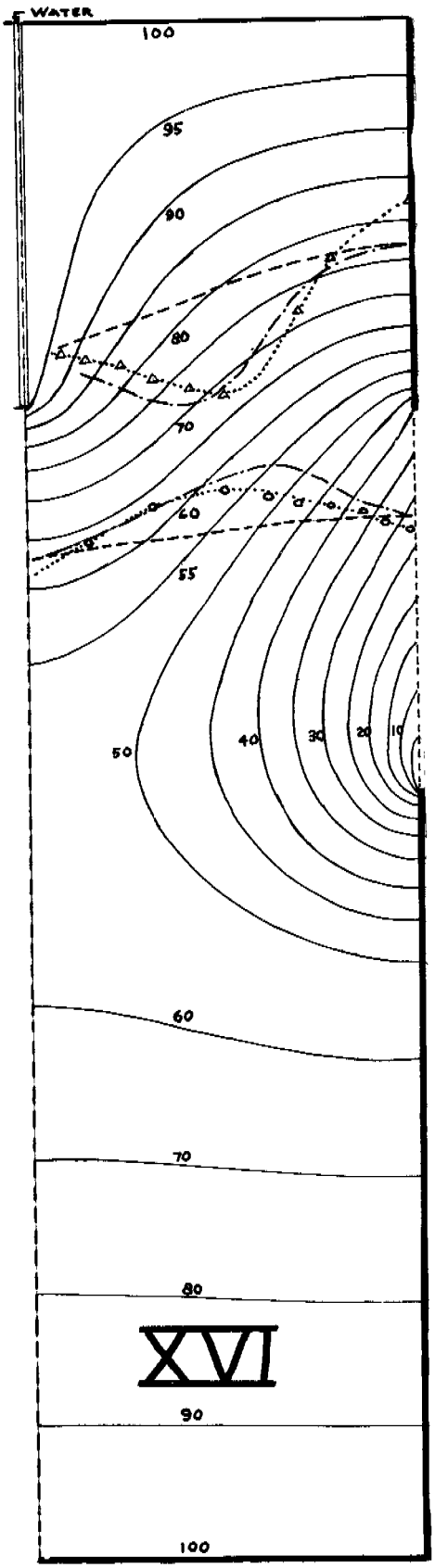
WATER
100
95
90
80
70
60
55
50
40
30
20
10
60
70
80
90
100
XVI

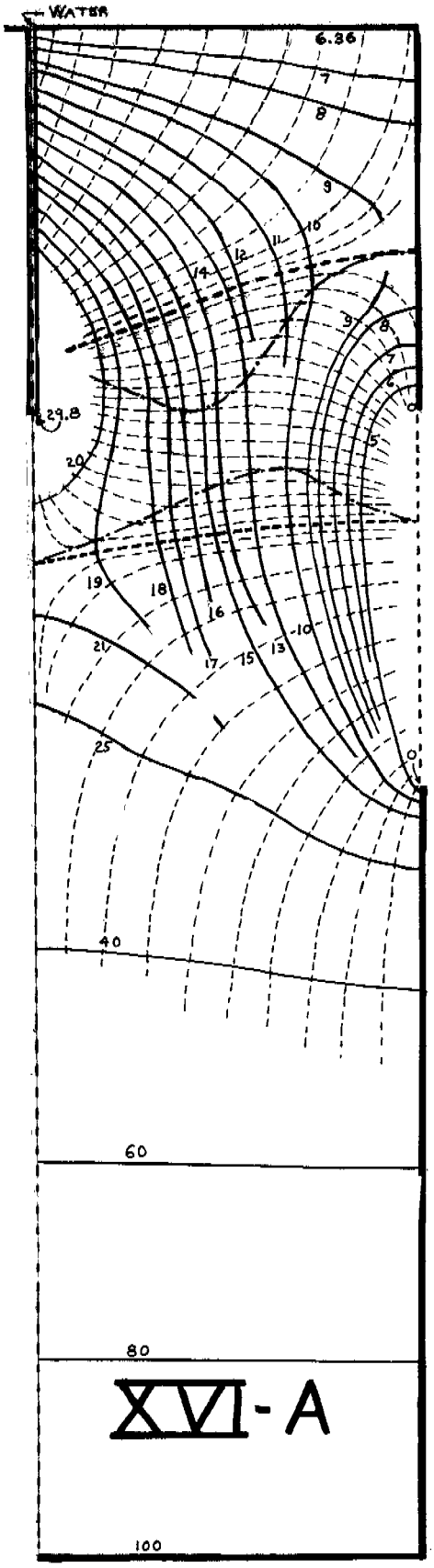
WATER
6.36
7
8
9
10
11
12
14
3
8
7
6
5
0
29.8
20
19
18
16
10
21
17
15
13
25
0
40
60
80
100
XVI-A

FIGURE 15

Open Drainage Port; Multiple Equidistant Slots; Pressure along Drainage Port is Less than Pressure above Column by the Equivalent of a Hydrostatic head T/2

Design	Depth of Cuts	W	T	D	L	V_i	V_b	Net Wash (e=0.5)
XVI (Fig. 11)	8	8	8	8	16	1.18	$1.62V_i$	45%
XVII	8, 4	8	8	8	16	1.20	$1.62V_i$	29%
XVIII	5, 4 1/2, 4, 3 1/2	8	8	8	16	1.44	$1.53V_i$	12.5%

...Δ...Δ...Δ...Δ...Δ...Δ... Mid-Point Locus for Approximate Upper Boundary of Wash Zone

...o...o...o...o...o...o... Mid-Point Locus Method for Projecting to Brine Peak at Center Line

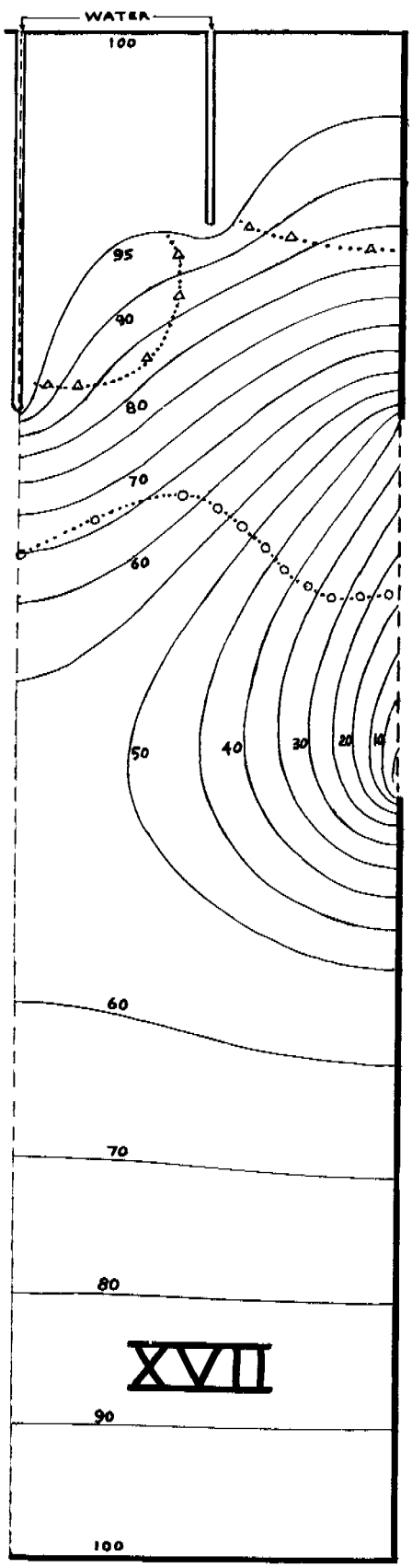
WATER
100
95
90
80
70
60
50
40
30
20
10
60
70
80
XVII
90
100

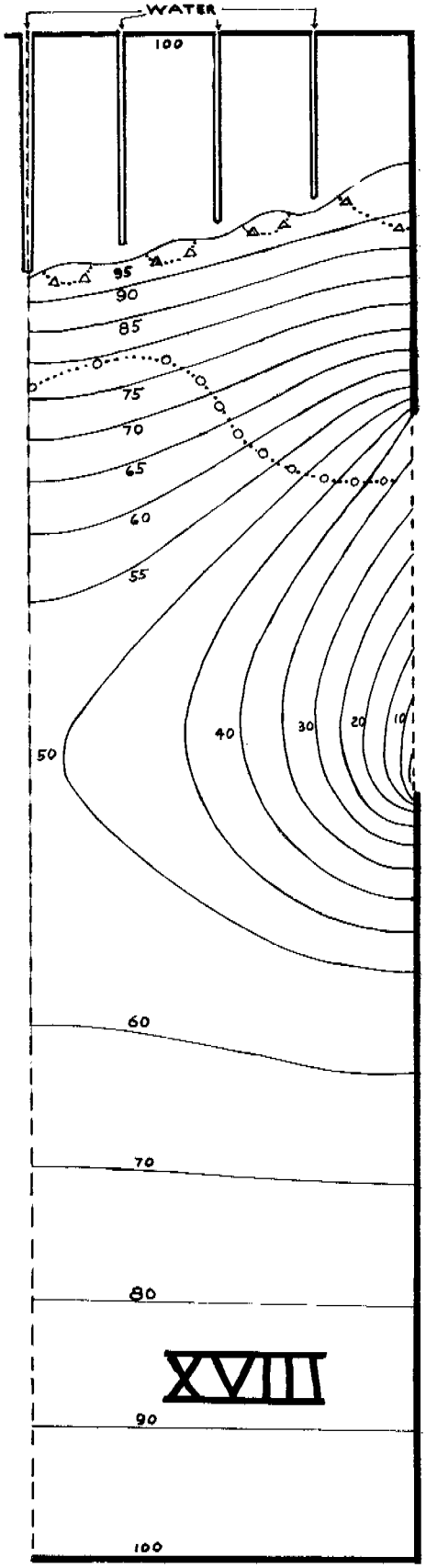
WATER
100
95
90
85
75
70
65
60
55
50
40
30
20
10
60
70
80
XVIII
90
100

LITERATURE CITED

(1) Albright, M. A., Complex Problems Solved with Models, Hydrocarbon Processing 43, 135 (July, 1964).

(2) Barduhn, A. J., Paper SWD/88, First International Symposium on Water Desalination, Washington, D. C., October 3-9 (1965).

(3) Bosworth, C. M., Barduhn, A. J., and D. J. Sandell, Advances in Chemistry Vol 27, 90 (1960), American Chemical Society, Washington D. C.

(4) Brandt, H. L., and B. M. Johnson, AIChE Journal 9, 771 (1963).

(5) Hahn, W. J., Burns, R. C., Fullerton, R. S., and D. J. Sandell, Development of the Direct Freeze Separation Process, Report to U. S. Dept. of Interior, Office of Saline Water, Res. and Dev. Prog. Rept. No. 113 (June, 1964).

(6) Johnson, C. A., Moore, S. J., Wagaman, N. D., and D. J. Sandell, Experimental Investigation of Direct Freeze Separation Process Using Refrigerant R - C318 (Octafluorocyclobutane), U. S. Dept. of Interior, Office of Saline Water, Res. and Dev. Prog. Rept. No. 256 (April, 1967).

(7) Karnofsky, G. Wash Column Design, Communication to Office of Saline Water (May 10, 1967).

(8) Karnofsky, G. Chem. Eng. Progress 57, 42 (January, 1960)

(9) Leinroth, J. P., White, W. P., Sherwood, T. K., and P. L. T. Brian, Washing of Brine from Ice Crystals, U. S. Dept. of Interior Office of Saline Water, Res. and Dev. Prog. Rept. No. 128, (January, 1965).

(10) Mixon, F. O., Calculation of Liquid Flow Rates in a Rectangular Wash-Separator Column with Vertical Filter Screens, Report to U. S. Dept. of Interior, Office of Saline Water (September 18, 1964).

(11) Sherwood, T. K., Brian, P. L. T., Sarofim, A. F., and K. A. Smith Research on Saline Water by Freezing, U. S. Dept. of Interior, Office of Saline Water, Res. and Dev. Prog Rept. No. 242 (March, 1967).

(12) Wiegandt, H. F., Advances in Chemistry, Vol 27, 82 (1960), American Chemical Society, Washington D. C.

(13) Wiegandt, H. F. and R. Lafay, IFP Process of Continuous Purification by Crystallization and Washing, Seventh World Petroleum Congress, Mexico City (April, 1967).

(14) Wiegandt, H. F. and P. Harriott, AIChE Journal 10, 755 (1964).

(15) Wiegandt, H. F., Power Generation in Combination with the Freezing Process for Saline Water Conversion, Report to the Office of Saline Water, September (1964).